PHYSICAL REVIEW D **84,** 074037 (2011)

Long-distance contribution to $\Delta\Gamma_s$ of the B_s-$\bar{B}_s$ system

Chun-Khiang Chua

Department of Physics, Chung Yuan Christian University, Chung-Li 32023, Taiwan, Republic of China

Wei-Shu Hou and Chia-Hsien Shen

Department of Physics, National Taiwan University, Taipei 10617, Taiwan, Republic of China, National Center for Theoretical Sciences, National Taiwan University, Taipei 10617, Taiwan, Republic of China

(Received 10 August 2011; published 31 October 2011)

We estimate the long-distance contribution to the width difference of the B_s-$\bar{B}_s$ system, based mainly on two-body $D_s^{(*)}\bar{D}_s^{(*)}$ modes and three-body $D_s^{(*)}\bar{D}^{(*)}\bar{K}^{(*)}$ modes (and their CP conjugates). Some higher $c\bar{s}$ resonances are also considered. The contribution to $\Delta\Gamma_s/\Gamma_s$ by two-body modes is $(10.2 \pm 3.0)\%$, slightly smaller than the short-distance result of $(13.3 \pm 3.2)\%$. The contribution to $\Delta\Gamma_s/\Gamma_s$ by $D_{s0}^*(2317)$, $D_{s1}(2460)$, and $D_{s1}(2536)$ resonances is negligible. For the three-body $D_s^{(*)}\bar{D}^{(*)}\bar{K}^{(*)}$ modes, we adopt the factorization formalism and model the form factors with off-shell $D_s^{(*)}$ poles, the $D_{sJ}(2700)$ resonance, and nonresonant contributions. These three-body modes can arise through current-produced or transition diagrams, but only SU(3)-related $D_{u,d}^{(*)}\bar{D}^{(*)}\bar{K}$ modes from the current diagram have been measured so far. The pole model results for $D_{u,d}^*\bar{D}^{(*)}\bar{K}$ agree well with the data, while $D_{u,d}\bar{D}^{(*)}\bar{K}$ rates agree with the data only within a factor of 2 to 3. All measured $D_{u,d}^{(*)}\bar{D}^{(*)}\bar{K}$ rates can be reproduced by including nonresonant contributions. The total $\Delta\Gamma_s/\Gamma_s$ obtained is $(16.7 \pm 8.5)\%$, which agrees with the short-distance result within uncertainties. For illustration, we also demonstrate the effect of $D_{sJ}(2700)$ in modes with $D^{(*)}K^*$. In all scenarios, the total $\Delta\Gamma_s/\Gamma_s$ remain consistent with the short-distance result. Our results indicate that (a) the operator product expansion in the short-distance picture is a valid assumption, (b) approximating the $B_s \to D_s^{(*)}\bar{D}_s^{(*)}$ decays to saturate $\Delta\Gamma_s$ has a large correction, (c) the effect of three-body modes cannot be neglected, and (d) in addition to the D_s and D_s^* poles, the $D_{sJ}(2700)$ resonance also plays an important role in three-body modes. Future experiments are necessary to improve the estimation of $\Delta\Gamma_s$ from the long-distance point of view.

DOI: 10.1103/PhysRevD.84.074037 PACS numbers: 11.30.Hv, 13.25.Hw, 14.40.Nd

I. INTRODUCTION AND MOTIVATION

One of the most exciting discoveries in particle physics last year was the anomalous like-sign dimuon charge asymmetry A_{sl}^b reported by the D0 Collaboration [1]. The updated result is $A_{sl}^b = (-0.787 \pm 0.172(\text{stat}) \pm 0.093(\text{syst}))\%$, based on 9.0 fb^{-1} data [2]. This result is 3.9σ larger than the standard model (SM) prediction of $(-0.024 \pm 0.003)\%$ [3]. This asymmetry comprises the wrong-sign asymmetries $a_{sl}^{d,s}$ for $B_{d,s}$ mesons [2,4],

$$A_{sl}^b = (0.594 \pm 0.022)a_{sl}^d + (0.406 \pm 0.022)a_{sl}^s. \quad (1)$$

From direct measurements by B factories [4], $a_{sl}^d = -(0.05 \pm 0.56)\%$ does not deviate from the SM prediction [3]. Imposing these two experimental values into Eq. (1), one finds a large a_{sl}^s. The very recent update used the muon-impact parameter to directly extract [2]

$$a_{sl}^d = -(0.12 \pm 0.52)\%, \qquad a_{sl}^s = -(1.81 \pm 1.06)\%. \quad (2)$$

The result of a_{sl}^s is much larger than the SM prediction of $(1.9 \pm 0.3) \times 10^{-5}$ [3]. The current world average of a_{sl}^s, obtained before the very recent update [2], is [4]

$$a_{sl}^s = -0.0115 \pm 0.0061, \quad (3)$$

which is still much larger than the SM prediction. This anomalous result has drawn intense theoretical attention, including model-independent analyses [5–9], and explanations from specific new-physics models [10–17].

The wrong-sign asymmetry a_{sl}^s can be derived from mixing parameters [1]

$$a_{sl}^s = \frac{\Delta\Gamma_s}{\Delta m_s}\tan\phi_s = \frac{2|\Gamma_{12,s}|}{\Delta m_s}\sin\phi_s, \quad (4)$$

where the $\Delta\Gamma_s$ and Δm_s are the width difference and mass difference of the B_s-$\bar{B}_s$ system, ϕ_s is the CP-violating phase, and $\Gamma_{12,s}$ is the absorptive off-diagonal element of the mixing matrix (see Sec. II A for more detail). Note that a_{sl}^s is bounded by $2|\Gamma_{12,s}|/\Delta m_s$. The short-distance calculation in the SM predicts [3],

$$\begin{aligned} \Delta\Gamma_{s,\text{SM}} &= (0.087 \pm 0.021)\ \text{ps}^{-1}, \\ \Delta\Gamma_{s,\text{SM}}/\Gamma_{s,\text{SM}} &= (13.3 \pm 3.2)\%, \\ \Delta m_{s,\text{SM}} &= (17.3 \pm 2.6)\ \text{ps}^{-1}, \\ \phi_{s,\text{SM}} &= (0.22^\circ \pm 0.06^\circ). \end{aligned} \quad (5)$$

Note that ϕ_s is very small in the SM, so $2|\Gamma_{12,s}| \cong |\Delta\Gamma_s|$. If one inserts Eq. (5) into Eq. (4), one gets the small value of a_{sl}^s mentioned before. These mixing parameters can be

measured independently. In particular, Δm_s has already been well-measured. The current world average is [4]

$$\Delta m_s = (17.78 \pm 0.12)\ \mathrm{ps}^{-1}, \tag{6}$$

which is consistent with the SM prediction. Using the experimental Δm_s and a^s_{sl}, Eq. (4) shows that $\Gamma_{12,s}$ has to be enhanced by at least 3 times the SM prediction. In fact, one of us has already pointed this out [18] in 2007, based on the earlier result of D0, which has almost the same central value as Ref. [1] but with larger uncertainty. Recent studies [5,6] also indicate this problem. On the other hand, $\Delta\Gamma_s$ and ϕ_s can also be measured in several ways, although the precision is not as good as Δm_s. One method to extract these values is to study the $B_s \to J/\psi\phi$ decay. D0 [19] reported

$$\begin{aligned}\Delta\Gamma_s &= +0.15 \pm 0.06(\mathrm{stat}) \pm 0.01(\mathrm{syst})\ \mathrm{ps}^{-1},\\ \phi_s &= -0.76^{+0.38}_{-0.36}(\mathrm{stat}) \pm 0.02(\mathrm{syst}),\end{aligned} \tag{7}$$

using 6.1 fb^{-1} of data. The consistency of data between mixing parameters (Δm_s, $\Delta\Gamma_s$, and ϕ_s) and a^s_{sl} has been observed [4,5]. Using almost the same amount of data, CDF [20] assumes $\phi_s = 0$ and reported

$$\Delta\Gamma_s = +0.075 \pm 0.035(\mathrm{stat}) \pm 0.01(\mathrm{syst})\ \mathrm{ps}^{-1}. \tag{8}$$

This central value drops to half the D0 result, even below the SM prediction. But the two results still agree with each other because the uncertainties so far are still large. The consistency hints that new physics may play a role in B_s-$\bar{B}_s$ mixing. New physics can easily enter the dispersive $M_{12,s}$ and the phase ϕ_s. On the other hand, $\Gamma_{12,s}$ is absorptive and thus hardly affected by new physics at the high energy scale. As very many properties of B mesons have been studied and found to agree with SM predictions, new physics has to be rather exotic to change $\Gamma_{12,s}$ while not affecting other known properties appreciably.

The absorptive nature of $\Gamma_{12,s}$ also makes the theoretical calculation challenging. It is helpful to revisit the calculation of $\Gamma_{12,s}$ in the SM. One either approximates $\Delta\Gamma_s$ by operator product expansion (OPE) in the short-distance picture, or estimates $\Delta\Gamma_s$ from several modes which are believed to be important. The SM prediction [3] mentioned previously adopts the short-distance scheme. On the other hand, Aleksan *et al.* [21] estimated $\Delta\Gamma_s$ from exclusive two-body decays, mainly, $D_s^{(*)}\bar{D}_s^{(*)}$ modes through color-allowed diagrams, as depicted in Fig. 1. Their result is close to the current SM prediction. They further pointed out that $\Delta\Gamma_s$ induced by $D_s^{(*)}\bar{D}_s^{(*)}$ modes approaches the result of the parton model when the limits $(m_b - 2m_c) \to 0$, $m_c \to \infty$ and the large N_c limit are simultaneously imposed. (For a detail discussion, see Ref. [22].) How well such an approximation holds in nature remains to be checked. For example, as Ref. [3] and one of us [18] have already pointed out, a 100% long-distance correction is possible. The large

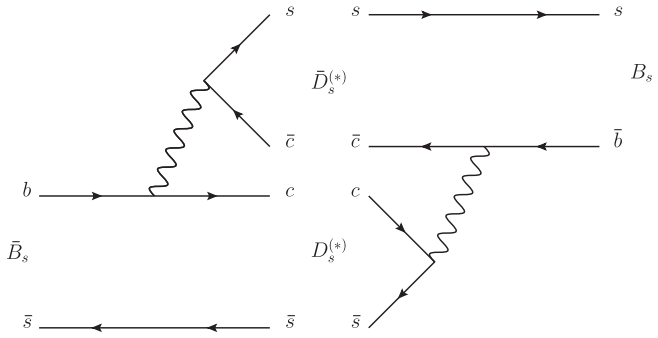

FIG. 1. The diagrams of B_s and $\bar{B}_s$ decay to $D_s^{(*)}\bar{D}_s^{(*)}$ modes.

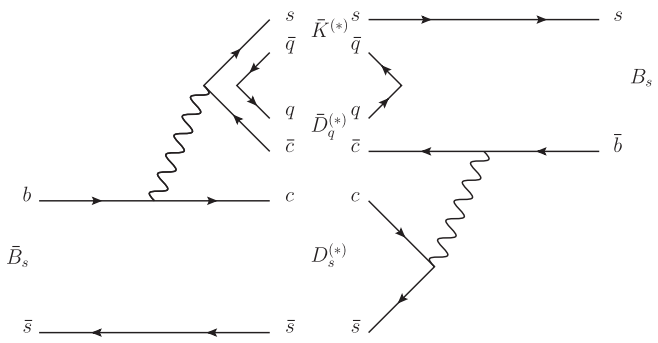

FIG. 2. The current and transition diagrams. Left: $\bar{B}_s \to D_s^{(*)}\bar{D}^{(*)}\bar{K}^{(*)}$, the current-produced diagram. Right: $B_s \to D_s^{(*)}\bar{D}^{(*)}\bar{K}^{(*)}$, the transition diagram.

a^s_{sl} therefore motivates one to investigate the long-distance effect. In this paper, we perform a detail estimation of $\Delta\Gamma_s$ from hadronic modes, which includes the two-body modes $D_s^{(*,**)}\bar{D}_s^{(*,**)}$, $D^{(*,**)}\bar{D}_{sJ}(2700)$, and the three-body $D^{(*)}\bar{D}^{(*)}\bar{K}^{(*)}$ modes.[1]

We give the first estimation of the contribution to $\Delta\Gamma_s$ by three-body $D_s^{(*)}\bar{D}^{(*)}\bar{K}^{(*)}$ modes (and their CP conjugates). We use the factorization approach, which seems to work well in color-allowed charmful three-body decays [23], in our calculations. As shown in Fig. 2, these modes can be produced by the diagram in Fig. 1, but with an extra $q\bar{q}$ pair produced either in the current or in the spectator part, which we denote as current-produced ($\mathcal{J}$) or transition ($\mathcal{T}$) modes. The number of $D_s^{(*)}\bar{D}^{(*)}\bar{K}$ channels is 4 times larger than $D_s^{(*)}\bar{D}_s^{(*)}$ modes, with a factor of 2 coming from extra $q\bar{q}$, which can be $u\bar{u}$ or $d\bar{d}$, and another two from the choice of $q\bar{q}$ in either current or transition processes. With this enhancement in number of modes, and if the branching fractions of these modes are not very small compared with the $D_s^{(*)}\bar{D}_s^{(*)}$ modes, it is natural to expect that $\Delta\Gamma_s$ may receive nonnegligible contributions from three-body $D_s^{(*)}\bar{D}^{(*)}\bar{K}^{(*)}$ modes. So far, the available measurements on these three-body modes are limited to

[1]Throughout this work, we use D_s^{**} to denote $D_{s0}^*(2317)$, $D_{s1}(2460)$, or $D_{s1}(2536)$.

current-produced modes with $\bar{K}$ in $\bar{B}_{u,d}$ systems only [24–28]. These modes are related to the corresponding modes in the $\bar{B}_s$ system under SU(3) symmetry. We need to reproduce existing three-body data before we make predictions for the $\bar{B}_s$ modes.

Let us briefly survey the experimental situation regarding the SU(3)-related three-body modes. There is no measurement of either transition modes or modes with $\bar{K}^*$. Despite a 2.2σ discrepancy on the branching fraction of $B^- \to D^0\bar{D}^0K^-$ decay between measurements [26,28], the branching fractions of current-produced $\bar{B}_{u,d} \to D^{(*)}_{u,d}\bar{D}^{(*)}\bar{K}$ modes are around 10^{-2} to 10^{-3}, 1 order of magnitude smaller compared to two-body modes. So far, $c\bar{s}$ resonances $\bar{D}_{s1}(2536)$ and $\bar{D}_{sJ}(2700)$ have been observed in the decays $\bar{B}_{u,d} \to D^{(*)}_{u,d}\bar{D}^{(*)}\bar{K}$ [25–27]. For the $D_{s1}(2536)$ resonance, its contribution to the branching fractions of three-body decays is on the order of 10^{-4}, which is small compared with the total branching fraction. On the other hand, Belle observed that $\bar{D}_{sJ}(2700)$ contributes to about half of the total branching fraction of $B^- \to D^0\bar{D}^0K^-$. Note that $D_{sJ}(2700)$ has a fairly broad width (~ 0.1 GeV). These measurements suggest that $D_{s1}(2536)$ could be treated in a two-body picture while it is more appropriate to consider $D_{sJ}(2700)$ in three-body decays. Furthermore, the contribution of $\bar{D}_{sJ}(2700)$ in $B^- \to D^0\bar{D}^0K^-$ decay is $\mathcal{B}(B^- \to D^0\bar{D}_{sJ}(2700)) \times \mathcal{B}(\bar{D}_{sJ}(2700) \to \bar{D}\,\bar{K}) = (0.113^{+0.026}_{-0.040})\%$, which is about half the total branching fraction $(0.222 \pm 0.033)\%$ [26]. Consequently, the contribution of $\bar{D}_{sJ}(2700)$ in three-body modes and in $\Delta\Gamma_s$ should be investigated.

This paper is organized as follows. In Sec. II, we describe our formalism and briefly review the newly discovered $D_{sJ}(2700)$ resonance that has a nonnegligible contribution to three-body modes. The results of two-body modes are discussed in Sec. III A. For three-body modes, we examine the factorization formalism and calculate $\Delta\Gamma_s$ in Sec. III B. Another scenario and the effect of four-body modes are discussed in Sec. IV, followed by the concluding section. Numerical inputs and some calculational details are collected in three Appendixes.

II. FORMALISM

A. Formula for $\Delta\Gamma$

The time evolution of a B_s meson can be described by the following formula,

$$i\frac{d}{dt}\begin{pmatrix}|B\rangle\\ |\bar{B}\rangle\end{pmatrix} = \left(M - i\frac{\Gamma}{2}\right)\begin{pmatrix}|B\rangle\\ |\bar{B}\rangle\end{pmatrix}, \tag{9}$$

in which we adopt the phase convention of $|B\rangle$ and $|\bar{B}\rangle$ to be $CP|B\rangle = -|\bar{B}\rangle$.[2] The Γ term in Eq. (9) is the absorptive part, which can be calculated by summing all on-shell intermediate states,

$$\Gamma_{ij} = \frac{1}{2M_B}\sum_f \int d\Phi\, \mathcal{A}^*_{B_i\to f}(\Phi)\mathcal{A}_{B_j\to f}(\Phi), \tag{10}$$

where Φ is over phase space variables.[3]

We define the width difference $\Delta\Gamma_s$ as the difference between light and heavy eigenstates, $\Gamma_L - \Gamma_H$. Assuming CP conservation, which is a good approximation for SM in the B_s-$\bar{B}_s$ system, the eigenstates of B_s meson are CP even and odd states. From the short-distance calculation of SM, the light and heavy eigenstates correspond to CP even and odd states, respectively. Thus, the $\Delta\Gamma_s$ can be related to Γ_{ij} by

$$\begin{aligned}\Delta\Gamma &\equiv \Gamma_L - \Gamma_H = -2\Gamma_{12}\\ &= -2\times\frac{1}{2M_B}\sum_f \int d\Phi\, \mathcal{A}^*_{B\to f}(\Phi)\mathcal{A}_{\bar{B}\to f}(\Phi),\end{aligned} \tag{11}$$

in which we have used $\Gamma_{21} = \Gamma^*_{12}$ from CPT symmetry, and $\Gamma_{12} = \Gamma^*_{12} = \mathrm{Re}(\Gamma_{12})$ from CP symmetry. The fact that Γ_{12} is real under CP symmetry can be seen from

$$\begin{aligned}\Gamma_{12} &= \frac{1}{2M_B}\sum_f \int d\Phi\, \mathcal{A}^*_{B\to f}(\Phi)\mathcal{A}_{\bar{B}\to f}(\Phi)\\ &= \frac{1}{2M_B}\sum_f \frac{1}{2}\int d\Phi(\mathcal{A}^*_{B\to f}(\Phi)\mathcal{A}_{\bar{B}\to f}(\Phi)\\ &\quad + \mathcal{A}^*_{B\to \bar{f}}(\Phi)\mathcal{A}_{\bar{B}\to \bar{f}}(\Phi))\\ &= \frac{1}{2M_B}\sum_f \mathrm{Re}\left[\int d\Phi\, \mathcal{A}^*_{B\to f}(\Phi)\mathcal{A}_{\bar{B}\to f}(\Phi)\right].\end{aligned} \tag{12}$$

The amplitude product $\mathcal{A}^*_{B\to f}(\Phi)\mathcal{A}_{\bar{B}\to f}(\Phi)$ is complex conjugate to the amplitude product of conjugate intermediate state $\mathcal{A}^*_{B\to \bar{f}}(\Phi)\mathcal{A}_{\bar{B}\to \bar{f}}(\Phi)$ by CP symmetry. Γ_{12} sums up all the intermediate states and turns out to be real. For convenience, we define the width difference of each exclusive decay as $\Delta\Gamma_f$, and its corresponding complex term in Γ_{12} to be

$$\Delta\Gamma_f \equiv -2\times \mathrm{Re}[\Gamma_{12,f}], \tag{13}$$

where $\Gamma_{12,f}$ is defined as

$$\Gamma_{12,f} \equiv \frac{1}{2M_B}\int d\Phi\, \mathcal{A}^*_{B\to f}(\Phi)\mathcal{A}_{\bar{B}\to f}(\Phi). \tag{14}$$

Although $\Gamma_{12,f}$ is complex by looking at one mode, the imaginary part is cancelled by its CP conjugate mode, and thus the total Γ_{12} turns out to be real. Once $\mathcal{A}_{B\to f}(\Phi)$ and $\mathcal{A}_{\bar{B}\to f}(\Phi)$ are known, one can readily calculate the corresponding $\Delta\Gamma_f$ and branching fractions. In the next section, we will apply the factorization formalism to obtain these amplitudes.

[2]Our phase convention differs from that in Ref. [1].

[3]For n-particle mode, the phase space measure is $d\Phi = \prod_{j=1}^n \frac{dp_j^3}{2E_j}\times(2\pi)^4\delta^4(\sum_{j=1}^n p_j - p_B)$.

Before we move to model-dependent calculation, it is useful to extract some general limits of the magnitude of $\Delta\Gamma_f$ from Eq. (13). For an intermediate state $|f\rangle$, the magnitude of $\Delta\Gamma_f$ induced by this state is bounded by

$$\left|\frac{\Delta\Gamma_f}{\Gamma}\right| = \frac{1}{\Gamma}\cdot|\mathrm{Re}[2\Gamma_{12,f}]| \tag{15a}$$

$$\leq \frac{1}{\Gamma}\cdot|2\Gamma_{12,f}| \tag{15b}$$

$$\leq \frac{2}{\Gamma}\cdot\frac{1}{2M_B}\int d\Phi\sqrt{|\mathcal{A}_{\bar{B}\to f}(\Phi)|^2}\times\sqrt{|\mathcal{A}_{B\to f}(\Phi)|^2} \tag{15c}$$

$$\leq 2\times\sqrt{\mathcal{B}_{\bar{B}\to f}}\times\sqrt{\mathcal{B}_{B\to f}}. \tag{15d}$$

There are three inequalities in this formula. The first inequality reflects that $\Delta\Gamma_f$ is only proportional to the real part of $\Gamma_{12,f}$. The second inequality is obtained by the fact that the phase of the amplitude product $\mathcal{A}^*_{B\to f}(\Phi)\mathcal{A}_{\bar{B}\to f}(\Phi)$ may be different over the phase space, which would reduce the overall $|\Gamma_{12,f}|$. The last inequality accounts for the "mismatch" effect between $|\mathcal{A}_{B\to f}(\Phi)|$ and $|\mathcal{A}_{\bar{B}\to f}(\Phi)|$. Even when the branching fractions of $\bar{B}\to f$ and $B\to f$ are the same, the induced $\Delta\Gamma$ could be quite small if the decay probabilities of the two modes are highly mismatched in phase space. Note that the latter two limits are experimental observables. If the branching fractions of $\bar{B}\to f$ and $B\to f$ are measured, one could find the maximal magnitude of the corresponding $\Gamma_{12,f}$. The bound can be refined by the second inequality if the Dalitz plots of the two modes are available. But the $\Delta\Gamma_f$, which is proportional to the real part $\Gamma_{12,f}$, could be any value in the range of $-2|\Gamma_{12,f}|$ to $+|2\Gamma_{12,f}|$.

B. Factorization formalism

The relevant effective Hamiltonian for the $b\to c$ transition is

$$\mathcal{H}_{\mathrm{eff}} = \frac{G_F}{\sqrt{2}}V_{cb}V^*_{cs}[c_1(\mu)\mathcal{O}^c_1(\mu)+c_2(\mu)\mathcal{O}^c_2(\mu)], \tag{16}$$

where $c_i(\mu)$ are the Wilson coefficients, and V_{cb} and V_{cs} are the Cabibbo-Kobayashi-Maskawa (CKM) matrix elements. The four-quark operators $\mathcal{O}_i$ are products of two $V-A$ currents, i.e., $\mathcal{O}^c_1=(\bar{c}b)_{V-A}(\bar{s}c)_{V-A}$ and $\mathcal{O}^c_2=(\bar{s}b)_{V-A}(\bar{c}c)_{V-A}$.

With the factorization ansatz, the amplitudes for two-body $\bar{B}_s\to\mathcal{D}^{(*)}_s\bar{\mathcal{D}}^{(*)}_s$ decays are given by

$$\mathcal{A}(\bar{B}_s\to\mathcal{D}^{(*)}_s\bar{\mathcal{D}}^{(*)}_s) = \frac{G_F}{\sqrt{2}}V_{cb}V^*_{cs}a_1\langle\mathcal{D}^{(*)}_s|(\bar{c}b)_{V-A}|\bar{B}_s\rangle\times\langle\bar{\mathcal{D}}^{(*)}_s|(\bar{s}c)_{V-A}|0\rangle, \tag{17}$$

where the effective coefficients are expressed as $a_1=c_1+c_2/3$ if naïve factorization is used. Note that $\mathcal{D}^{(*)}_s$ could be the usual $D^{(*)}_s$ and/or a higher D_s resonance such as $D^*_{s0}(2317)$, $D_{s1}(2460)$, $D_{s1}(2536)$, and $D_{sJ}(2700)$. The factorized amplitudes consist of the products of two common matrix elements: the current-produced $\mathcal{D}^{(*)}_s$ and the $\bar{B}_s$-to-$\mathcal{D}^{(*)}_s$ transition. They are parametrized by the standard way [29]. The matrix elements of current-produced $\mathcal{D}^{(*)}_s$ are

$$\begin{aligned}\langle\mathcal{D}_s(p)|(V-A)_\mu|0\rangle &= if_{\mathcal{D}_s}p_\mu,\\ \langle\mathcal{D}^*_s(p,\lambda)|(V-A)_\mu|0\rangle &= m_{\mathcal{D}^*_s}f_{\mathcal{D}^*_s}\varepsilon^*_\mu(p,\lambda).\end{aligned} \tag{18}$$

The transition matrix elements for $\mathcal{D}^{(*)}_s$ are

$$\begin{aligned}&\langle\mathcal{D}_s(p_D)|(V-A)_\mu|\bar{B}_s(p_B)\rangle\\ &\quad=\left((p_B+p_D)_\mu-\frac{m^2_B-m^2_D}{q^2}q_\mu\right)F_1^{\bar{B}_s\mathcal{D}_s}(q^2)\\ &\qquad+\frac{m^2_B-m^2_D}{q^2}q_\mu F_0^{\bar{B}_s\mathcal{D}_s}(q^2),\\ &\langle\mathcal{D}^*_s(p_{D^*},\lambda)|(V-A)_\mu|\bar{B}_s(p_B)\rangle\\ &\quad=\epsilon_{\mu\nu\rho\sigma}\varepsilon^{*\nu}p^\rho_Bp^\sigma_{D^*}\cdot\frac{2F_3^{\bar{B}_s\mathcal{D}^*_s}(q^2)}{m_B+m_{D^*}}\\ &\qquad-i\left(\varepsilon^*_\mu-\frac{\varepsilon^*\cdot q}{q^2}q_\mu\right)(m_B+m_{D^*})F_1^{\bar{B}_s\mathcal{D}^*_s}(q^2)\\ &\qquad+i\left((p_B+p_{D^*})_\mu-\frac{m^2_B-m^2_{D^*}}{q^2}q_\mu\right)(\varepsilon^*\cdot q)\frac{F_2^{\bar{B}_s\mathcal{D}^*_s}(q^2)}{m_B+m_{D^*}}\\ &\qquad-i\frac{\varepsilon^*\cdot q}{q^2}q_\mu 2m_{D^*}F_0^{\bar{B}_s\mathcal{D}^*_s}(q^2),\end{aligned} \tag{19}$$

where $\epsilon_{\mu\nu\rho\sigma}$ is the totally antisymmetric symbol with $\epsilon_{0123}=1$. For convenience, our notations of decay constants and form factors of D^{**}_s are different from the usual notations. The conversion can be found in Appendix A.

The amplitudes of three-body modes $D^{(*)}\bar{D}^{(*)}\bar{K}^{(*)}$ decayed from $\bar{B}$ and B are given by

$$\begin{aligned}&\mathcal{A}_{\mathcal{J}}(\bar{B}_s\to D^{(*)}_s\bar{D}^{(*)}\bar{K}^{(*)})\\ &\quad=\frac{G_F}{\sqrt{2}}V_{cb}V^*_{cs}a_1\langle D^{(*)}_s|(\bar{c}b)_{V-A}|\bar{B}_s\rangle\cdot\langle\bar{D}^{(*)}\bar{K}^{(*)}|(\bar{s}c)_{V-A}|0\rangle,\\ &\mathcal{A}_{\mathcal{T}}(B_s\to D^{(*)}_s\bar{D}^{(*)}\bar{K}^{(*)})\\ &\quad=\frac{G_F}{\sqrt{2}}V_{cb}V^*_{cs}a_1\langle\bar{D}^{(*)}\bar{K}^{(*)}|(\bar{c}b)_{V-A}|B_s\rangle\cdot\langle D^{(*)}_s|(\bar{s}c)_{V-A}|0\rangle,\end{aligned} \tag{20}$$

where $\mathcal{A}_{\mathcal{J}}$ and $\mathcal{A}_{\mathcal{T}}$ denote the amplitudes of current and transition diagrams, respectively. Unlike the $\mathcal{D}^{(*)}_s\bar{\mathcal{D}}^{(*)}_s$ modes in which only standard form factors appear, these amplitudes involve the timelike form factors and transition form factors of two pseudoscalars ($\bar{D}\bar{K}$) or vectors ($\bar{D}^*\bar{K}^*$), or a pseudoscalar with a vector ($\bar{D}^*\bar{K}$ or $\bar{D}\bar{K}^*$).

The parametrization of timelike form factors is similar to the spacelike counterparts, such as $\langle D_s^{(*)}|V-A|\bar{B}_s\rangle$. The timelike form factors of two pseudoscalars (PP) states are given by

$$\begin{aligned}\langle P_a(p_a)P_b(p_b)|(V-A)_\mu|0\rangle &= \left((p_a-p_b)_\mu - \frac{m_a^2-m_b^2}{q^2}q_\mu\right)F_1^{PP}(q^2) \\ &+ \frac{m_a^2-m_b^2}{q^2}q_\mu F_0^{PP}(q^2),\end{aligned} \tag{21}$$

where $q^\mu = p_a^\mu + p_b^\mu$ is the momentum of the current. For the states with one vector and pseudoscalar (VP), the parametrization of timelike form factors is

$$\begin{aligned}&\langle V(p_V,\varepsilon_V)P(p_P)|(V-A)_\mu|0\rangle \\ &= -\epsilon_{\mu\nu\rho\sigma}\varepsilon_V^{*\nu}p_P^\rho p_V^\sigma\cdot\frac{2V^{VP}(q^2)}{m_V+m_P} \\ &- i\left(\varepsilon_{V\mu}^* - \frac{\varepsilon_V^*\cdot q}{q^2}q_\mu\right)(m_V+m_P)A_1^{VP}(q^2) \\ &- i\left((p_V-p_P)_\mu - \frac{m_V^2-m_P^2}{q^2}q_\mu\right)(\varepsilon_V^*\cdot q)\frac{A_2^{VP}(q^2)}{m_V+m_P} \\ &- i\frac{\varepsilon_V^*\cdot q}{q^2}q_\mu 2m_V A_0^{VP}(q^2).\end{aligned} \tag{22}$$

The timelike form factors of two-vector (VV) states can be parameterized analogously,

$$\begin{aligned}\langle V_a(p_a,\varepsilon_a)V_b(p_b,\varepsilon_b)|(V-A)_\mu|0\rangle &= i\epsilon_{\alpha\nu\rho\sigma}\varepsilon_b^{*\alpha}\varepsilon_a^{*\nu}p_a^\rho p_b^\sigma q_\mu\frac{V_0^{VV}(q^2)}{(m_a+m_b)^2} + i\epsilon_{\mu\nu\rho\sigma}\varepsilon_a^{*\nu}p_a^\rho p_b^\sigma(\varepsilon_b^*\cdot q)\frac{V_1^{VV}(q^2)}{(m_a+m_b)^2} \\ &+ i\epsilon_{\mu\nu\rho\sigma}\varepsilon_b^{*\nu}p_a^\rho p_b^\sigma(\varepsilon_a^*\cdot q)\frac{V_2^{VV}(q^2)}{(m_a+m_b)^2} + \left(\varepsilon_{a\mu}^* - \frac{\varepsilon_a^* q}{q^2}q_\mu\right)(\varepsilon_b^*\cdot q)A_{11}^{VV}(q^2) \\ &+ \left(\varepsilon_{b\mu}^* - \frac{\varepsilon_b^*\cdot q}{q^2}q_\mu\right)(\varepsilon_a^*\cdot q)A_{12}^{VV}(q^2) + \left((p_a-p_b)_\mu - \frac{m_a^2-m_b^2}{q^2}q_\mu\right)(\varepsilon_a^*\cdot\varepsilon_b^*)A_2^{VV}(q^2) \\ &+ (\varepsilon_a^*\cdot q)(\varepsilon_b^*\cdot q)\frac{q_\mu}{q^2}A_{01}^{VV}(q^2) + (\varepsilon_a^*\cdot\varepsilon_b^*)\frac{q_\mu}{q^2}(m_a+m_b)^2A_{02}^{VV}(q^2).\end{aligned} \tag{23}$$

The transition form factors are more complicated. The cases of B_s to PP transition form factors were formulated in a general way in Ref. [30], which can be rewritten as

$$\begin{aligned}\langle P_a(p_a)P_b(p_b)|(V-A)_\mu|\bar{B}_s(p_B)\rangle &= \epsilon_{\mu\nu\rho\sigma}p_B^\nu q^\rho(p_a-p_b)^\sigma\frac{V^{\bar{B}_sPP}}{m_{B_s}^3} + i\left((p_B+q)_\mu - \frac{m_{B_s}^2-q^2}{q'^2}q'_\mu\right)\frac{A_1^{\bar{B}_sPP}}{m_{B_s}} \\ &+ i\left((p_a-p_b)_\mu - \frac{m_a^2-m_b^2}{q^2}q_\mu\right)\frac{A_2^{\bar{B}_sPP}}{m_{B_s}} + i\frac{m_a^2-m_b^2}{q^2}q_\mu\frac{A_0^{\bar{B}_sPP}}{m_{B_s}},\end{aligned} \tag{24}$$

where $q^\mu = p_a^\mu + p_b^\mu$ is the total momentum of PP, and $q'^\mu = p_B^\mu - q^\mu$ is the momentum of the external current. In this form, the terms with A_1 and A_2 are zeros when contracted with q' and q. For the transition form factors of $\bar{B}_s$ to VP and VV, since they are more complicated and there is so far no data, we only write down the form factors obtained from the pole model rather than the general forms. For VP, we have

$$\begin{aligned}\langle V(p_V,\varepsilon_V)P(p_P)|(V-A)^\mu|\bar{B}_s(p_B)\rangle &= i\epsilon_{\alpha\nu\rho\sigma}\left(-g^{\mu\alpha} + \frac{q'^\mu q'^\alpha}{q'^2}\right)\varepsilon_V^{*\nu}p_P^\rho p_V^\sigma\frac{V_2^{\bar{B}_sVP}}{m_{\bar{B}_s}^2} + i\epsilon_{\alpha\nu\rho\sigma}q'^\alpha\varepsilon_V^{*\nu}p_P^\rho p_V^\sigma\left((p_B+q)^\mu\right. \\ &\left. - \frac{m_{B_s}^2-q^2}{q'^2}q'^\mu\right)\frac{V_1^{\bar{B}_sVP}}{m_{B_s}^4} + i\epsilon_{\alpha\nu\rho\sigma}q'^\alpha\varepsilon_V^{*\nu}p_P^\rho p_V^\sigma\frac{q'^\mu}{q'^2}\frac{V_0^{\bar{B}_sVP}}{m_{\bar{B}_s}^2} \\ &+ \epsilon_{\alpha\beta\gamma\delta}\epsilon_{abcd}(g^{\mu\alpha}g^{\beta a})q'^\gamma q^\delta\varepsilon_V^{*b}p_P^c p_V^d\frac{A_3^{\bar{B}_sVP}}{m_{B_s}^4} \\ &+ \left((p_B+q)^\mu - \frac{m_{B_s}^2-q^2}{q'^2}q'^\mu\right)(\varepsilon_V^*\cdot q)\frac{A_1^{\bar{B}_sVP}}{m_{\bar{B}_s}^2} + \frac{m_{B_s}^2-q^2}{q'^2}q'^\mu(\varepsilon_V^*\cdot q)\frac{A_0^{\bar{B}_sVP}}{m_{\bar{B}_s}^2},\end{aligned} \tag{25}$$

and for $\bar{B}_s$ to VV, we parametrize as

$$
\begin{aligned}
&\langle V_a(p_a,\varepsilon_a)V_b(p_b)|(V-A)_\mu|\bar{B}_s(p_B)\rangle \\
&= \epsilon_{\mu\nu\rho\sigma}p_a^\nu p_b^\rho q'^\sigma(\varepsilon_a^*\cdot\varepsilon_b^*)\frac{V_3^{\bar{B}_sVV}}{m_{B_s}^3}+\epsilon_{\mu\nu\rho\sigma}\varepsilon_a^{*\nu}q'^\rho q^\sigma(\varepsilon_b^*\cdot q)\frac{V_2^{\bar{B}_sVV}}{m_{B_s}^3}+\epsilon_{\mu\nu\rho\sigma}\varepsilon_b^{*\nu}q'^\rho q^\sigma(\varepsilon_a^*\cdot q)\frac{V_1^{\bar{B}_sVV}}{m_{B_s}^3} \\
&+\epsilon_{\alpha\nu\rho\sigma}\varepsilon_b^{*\alpha}\varepsilon_a^{*\nu}p_a^\rho p_b^\sigma\left((p_B+q)_\mu-\frac{m_{B_s}^2-q^2}{q'^2}q'_\mu\right)\frac{V_{01}^{\bar{B}_sVV}}{m_{B_s}^3}+\epsilon_{\alpha\nu\rho\sigma}\varepsilon_b^{*\alpha}\varepsilon_a^{*\nu}p_a^\rho p_b^\sigma\frac{m_{B_s}^2-q^2}{q'^2}q'_\mu\frac{V_{00}^{\bar{B}_sVV}}{m_{B_s}^3} \\
&+i(\varepsilon_a^*\cdot\varepsilon_b^*)\left((p_a-p_b)_\mu-\frac{m_a^2-m_b^2}{q'^2}q'_\mu\right)\frac{A_{62}^{\bar{B}_sVV}}{m_{B_s}}+i(\varepsilon_a^*\cdot\varepsilon_b^*)\left((p_B+q)_\mu-\frac{m_{B_s}^2-q^2}{q'^2}q'_\mu\right)\frac{A_{61}^{\bar{B}_sVV}}{m_{B_s}} \\
&+i(\varepsilon_a^*\cdot\varepsilon_b^*)\frac{q'_\mu}{q'^2}m_{B_s}A_{60}^{\bar{B}_sVV}+i(\varepsilon_b^*\cdot q)\left(\varepsilon_{a\mu}^*-\frac{\varepsilon_a^*q}{q^2}q_\mu\right)\frac{A_3^{\bar{B}_sVV}}{m_{B_s}}+i(\varepsilon_a^*\cdot q)\left(\varepsilon_{b\mu}^*-\frac{\varepsilon_b^*q}{q^2}q_\mu\right)\frac{A_4^{\bar{B}_sVV}}{m_{B_s}} \\
&+i(\varepsilon_a^*\cdot q')(\varepsilon_b^*\cdot q)\left((p_B+q)_\mu-\frac{m_{B_s}^2-q^2}{q'^2}q'_\mu\right)\frac{A_{21}^{\bar{B}_sVV}}{m_{B_s}^3}+i(\varepsilon_a^*\cdot q')(\varepsilon_b^*\cdot q)\frac{q'_\mu}{q'^2}\frac{A_{20}^{\bar{B}_sVV}}{m_{B_s}} \\
&+i(\varepsilon_a^*\cdot q)(\varepsilon_b^*\cdot q')\left((p_B+q)_\mu-\frac{m_{B_s}^2-q^2}{q'^2}q'_\mu\right)\frac{A_{11}^{\bar{B}_sVV}}{m_{B_s}^3}+i(\varepsilon_a^*\cdot q)(\varepsilon_b^*\cdot q')\left(\frac{q'_\mu}{q'^2}\right)\frac{A_{10}^{\bar{B}_sVV}}{m_{B_s}} \\
&+i(\varepsilon_a^*\cdot q)(\varepsilon_b^*\cdot q)\left((p_B+q)_\mu-\frac{m_{B_s}^2-q^2}{q'^2}q'_\mu\right)\frac{A_{01}^{\bar{B}_sVV}}{m_{B_s}^3}+i(\varepsilon_a^*\cdot q)(\varepsilon_b^*\cdot q)\frac{q'_\mu}{q'^2}\frac{A_{00}^{\bar{B}_sVV}}{m_{B_s}}.
\end{aligned}
\tag{26}
$$

Under CP conservation, all these form factors can be related to the form factors of their CP conjugates. These transformations are provided in Appendix A.

C. Pole model

Since the branching fractions of $D_s^{(*)}\bar{D}_s^{(*)}$ are large, it is natural to expect a sizable contribution from off-shell $D_s^{(*)}$ poles. In addition, experiments have observed $D_{sJ}(2700)$ in the three-body decays, as we have described in the introduction [25,26]. $D_{sJ}(2700)$ can decay to on-shell $D^{(*)}K$, but only goes off shell to $D^{(*)}K^*$ because of kinematics. As shown in Fig. 3, we consider pole exchanges, including D_s, D_s^*, and $D_{sJ}(2700)$, in three-body decays. Note that the D_s pole goes only to D^*K rather than to DK.

In the following calculation, we use off-shell $D_s^{(*)}$ poles and $D_{sJ}(2700)$ to model the $D^{(*)}K^{(*)}$ form factors. The effective Lagrangian taken from Refs. [31–33] is applied to describe the interaction between $D_q^{(*)}$ mesons and light pseudoscalar or vector mesons. The pole contribution to $D^{(*)}K^{(*)}$ form factors can be calculated by

$$
\begin{aligned}
\langle D^{(*)}K^{(*)}|(V-A)_\mu|0\rangle_{\rm pole} &= \frac{i}{q^2-m_{\rm int}^2+im_{\rm int}\Gamma_{\rm int}}\times\langle D^{(*)}K^{(*)}|i\mathcal{L}_{\rm eff}|D_{\rm int}\rangle\langle D_{\rm int}|(V-A)_\mu|0\rangle \\
&+\frac{i}{q^2-m_{\rm int*}^2+im_{\rm int*}\Gamma_{\rm int*}}\left(-g^{\alpha\beta}+\frac{q^\alpha q^\beta}{m_{\rm int*}^2}\right) \\
&\times\frac{\partial^2}{\partial\varepsilon_{\rm int}^{*\alpha}\partial\varepsilon_{\rm int}^\beta}(\langle D^{(*)}K^{(*)}|i\mathcal{L}_{\rm eff}|D_{\rm int}^*\rangle\langle D_{\rm int}^*|(V-A)_\mu|0\rangle), \\
\langle D^{(*)}K^{(*)}|(V-A)_\mu|\bar{B}\rangle_{\rm pole} &= \frac{i}{q^2-m_{\rm int}^2+im_{\rm int}\Gamma_{\rm int}}\times\langle D^{(*)}K^{(*)}|i\mathcal{L}_{\rm eff}|D_{\rm int}\rangle\langle D_{\rm int}|(V-A)_\mu|\bar{B}\rangle \\
&+\frac{i}{q^2-m_{\rm int*}^2+im_{\rm int*}\Gamma_{\rm int*}}\times\left(-g^{\alpha\beta}+\frac{q^\alpha q^\beta}{m_{\rm int*}^2}\right) \\
&\times\frac{\partial^2}{\partial\varepsilon_{\rm int}^{*\alpha}\partial\varepsilon_{\rm int}^\beta}(\langle D^{(*)}K^{(*)}|i\mathcal{L}_{\rm eff}|D_{\rm int}^*\rangle\langle D_{\rm int}^*|(V-A)_\mu|\bar{B}\rangle),
\end{aligned}
\tag{27}
$$

where the $D_{\rm int}^{(*)}$ is the intermediate particle with mass $m_{\rm int(*)}$ and width $\Gamma_{\rm int(*)}$. We adopt the Breit-Wigner form of the propagator and replace $\varepsilon_{\rm int}^{*\alpha}\varepsilon_{\rm int}^\beta$ with $(-g^{\alpha\beta}+q^\alpha q^\beta/m_{\rm int*}^2)$ to account for the off-shell effect. The explicit forms of the matrix elements $\langle D^{(*)}K^{(*)}|i\mathcal{L}_{\rm eff}|D_{\rm int}^{(*)}\rangle$ in the above equations can be found in Ref. [33]. A full list of pole contributions to form factors is listed in Appendix B.

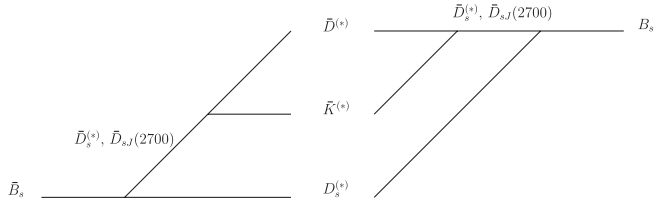

FIG. 3. Pole diagram of $\bar{B}_s$-B_s mixing. Left: the current-produced diagram. Right: the transition diagram.

D. $D_{sJ}(2700)$ resonance

The relevant properties and parameters of $D_{sJ}(2700)$ are summarized in this section. The mass and width of this resonance are [34]

$$\begin{aligned} m_{D_{sJ}(2700)} &= 2709^{+9}_{-6}\ \text{MeV}, \\ \Gamma_{D_{sJ}(2700)} &= 125 \pm 30\ \text{MeV}. \end{aligned} \tag{28}$$

Note that the width has a large uncertainty ($\sim 25\%$). The ratio of branching fractions of this resonance to DK and D^*K is also measured [35],

$$\begin{aligned} r(D^*K) &\equiv \frac{\mathcal{B}(D_{sJ}(2700)^+ \to D^*K)}{\mathcal{B}(D_{sJ}(2700)^+ \to DK)} \\ &= 0.91 \pm 0.13_{\text{stat}} \pm 0.12_{\text{syst}}, \end{aligned} \tag{29}$$

where $D^{(*)}K$ is the average of $D^{(*)}K_S$ and $D^{(*)}K^+$ modes. On the other hand, the contribution of $D_{sJ}(2700)$ in the decay $B^+ \to \bar{D}^0 D^0 K^+$, denoted as $\mathcal{B}(B^+ \to \bar{D}^0 D_{sJ}(2700)) \times \mathcal{B}(D_{sJ}(2700) \to D^0 K^+)$, is extracted [26],

$$\begin{aligned} &\mathcal{B}(B^+ \to \bar{D}^0 D_{sJ}(2700)) \times \mathcal{B}(D_{sJ}(2700) \to DK) \\ &\quad = (11.3^{+2.6}_{-4.0}) \times 10^{-4}, \end{aligned} \tag{30}$$

which constitutes about half the total branching fraction of this measurement. Note that this quantity has a large uncertainty, similar to the measurement of width. The quantum number of $D_{sJ}(2700)$ is determined to be $J^P = 1^-$ from the helicity angle distribution, which limits this resonance to be either an s-wave or a d-wave meson (or a mixed state between them). The interpretation of $D_{sJ}(2700)$ as a radial excitation of D_s^* ($n^{2S+1}L_J = 2^3S_1$) is proposed, which can explain its mass [36], partial width [37], and contribution to $B^+ \to \bar{D}^0 D^0 K^+$ decay [38]. In some strong decay models, a mixed state $2^3S_1 - 1^3D_1$ describes the partial width better [39]. As the theoretical predictions of mass and partial width are highly model-dependent, the identification is still not clear yet. We assume $D_{sJ}(2700)$ as a 2^3S_1 state in this study.

The effective Lagrangian in Refs. [31–33] can still be applied to describe the interaction between $D_{sJ}(2700)$ and light mesons [37]. We work out the relevant matrix elements,

$$\begin{aligned} &\langle D(p_2)K(p_3)|i\mathcal{L}_{\text{eff}}|D_{sJ}(2700)(p_1,\varepsilon_1)\rangle \\ &\quad = -i\tilde{g}_{D_{sJ}DK}\varepsilon_1 \cdot p_3, \\ &\langle D^*(p_2,\varepsilon_2)K(p_3)|i\mathcal{L}_{\text{eff}}|D_{sJ}(2700)(p_1,\varepsilon_1)\rangle \\ &\quad = -i\tilde{g}_{D_{sJ}D^*K}\epsilon_{\mu\nu\alpha\beta}\varepsilon_1^\mu \varepsilon_2^{*\nu} p_3^\alpha p_1^\beta, \end{aligned} \tag{31}$$

where the strong coupling constants are given by Ref. [37],

$$\tilde{g}_{D_{sJ}DK} = 2\frac{\tilde{g}}{f_\pi}\sqrt{m_{D_{sJ}} m_D}, \qquad \tilde{g}_{D_{sJ}D^*K} = 2\frac{\tilde{g}}{f_\pi}\sqrt{\frac{m_{D^*}}{m_{D_{sJ}}}}, \tag{32}$$

with $f_\pi = 132$ MeV. Once the coupling constants and form factors are extracted, one can insert Eq. (31) into Eq. (27) to obtain the contribution to form factors from the $D_{sJ}(2700)$ resonance.

From these matrix elements, Ref. [37] predicted the ratio of branching fractions

$$r(D^*K) = 0.91 \pm 0.04. \tag{33}$$

This ratio agrees with Eq. (29) very well. The ratios of the branching fractions of the six main decay modes are given in Table I. The mixing angle between η and η' is taken from Ref. [40].

Assuming $D_{sJ}(2700)$ decays only to $D^{(*)}K$ and $D^{(*)}\eta^{(\prime)}$, $\tilde{g}^2$ is proportional to the total width. Thus, we have

$$\tilde{g} = 0.28 \pm 0.03, \tag{34}$$

where the uncertainty comes from the uncertainty of the total width. Note that this value is slightly larger than the one in Ref. [37] as the world average of width [Eq. (28)] became larger.

Taking the measured mass, width, and $\mathcal{B}(B \to \bar{D}^{(*)} D_{sJ}(2700)) \times \mathcal{B}(D_{sJ}(2700) \to DK)$ (see Sec. III B for details) as input, the $D_{sJ}(2710)$ decay constant is extracted as

$$f_{D_{sJ}(2700)} = 240 \pm 31\ \text{MeV}. \tag{35}$$

The decay constant can be compared to the previous estimations 243 ± 41 MeV in Ref. [37] and 295 ± 13 MeV in Ref. [38]. Note that it is compatible with the decay constants of $D_s^{(*)}$, for which we use 260 ± 13 MeV in a later calculation.

The $\bar{B}_s \to D_{sJ}(2700)$ transition form factors can be obtained by using a covariant light-front quark model [33]. For the $2S$ wave function,[4] its Gaussian width can be fixed by the decay constant derived from Eq. (30). It is

[4]In the quark model with a simple harmonic-like potential, the wave function for a state with the quantum numbers (n, l, m) is given by $f_{nl}(\vec{p}^2/\beta^2)Y_{lm}(\hat{p})\exp(-\vec{p}^2/2\beta)$ with $f_{10}(x) = 1$ and $f_{20}(x) = \sqrt{\frac{3}{2}}(-1 + \frac{2}{3}x)$. We fit the Gaussian width β to the decay constant.

TABLE I. The ratio r of the branching fractions of six main decay modes of the $D_{sJ}(2700)^+$ resonance.

Mode(f)	D^0K^+	$D^+\bar{K}^0$	$D^{*0}K^+$	$D^{*+}\bar{K}^0$	$D_s\eta$	$D_s^*\eta$
$r(f)$	1.02	0.98	0.93	0.89	0.17	0.04

then straightforward to obtain various $\bar{B}_s \to D_{sJ}$ form factors:

$$\begin{aligned} V^{\bar{B}_s D_{sJ}(2700)}(q^2) &= \frac{0.25 \pm 0.03}{1 - 0.03q^2/m_{B_s}^2 + 0.38q^4/m_{B_s}^4}, \\ A_0^{\bar{B}_s D_{sJ}(2700)}(q^2) &= \frac{0.24 \pm 0.02}{1 + 1.16q^2/m_{B_s}^2 + 2.16q^4/m_{B_s}^4}, \\ A_1^{\bar{B}_s D_{sJ}(2700)}(q^2) &= \frac{0.17 \pm 0.02}{1 + 0.66q^2/m_{B_s}^2 + 0.54q^4/m_{B_s}^4}, \\ A_2^{\bar{B}_s D_{sJ}(2700)}(q^2) &= \frac{0.007 \pm 0.001}{1 + 4.84q^2/m_{B_s}^2 + 5.08q^4/m_{B_s}^4}. \end{aligned} \tag{36}$$

These transition form factors are small compared to the $D_s^{(*)}$ (collected in Appendix A), because of the poor overlap between wave functions of ground state B mesons and the radial excited $D_{sJ}(2700)$.

E. Nonresonance contribution

In general, there will be both resonant and nonresonant (NR) contributions to form factors. According to previous study of $\bar{B} \to D^{(*)}K^-K^0$ decays [23], it is necessary to add the NR contribution to form factors to explain the experimental observations. Therefore, we should include the NR effect in this work. To produce the $D^{(*)}K^{(*)}$ pairs, at least one gluon must be emitted to produce $q\bar{q}$ pairs. The QCD counting rule [23] provides an ansatz for the asymptotic behavior of the nonresonant form factors, which is

$$F(q^2)_{\rm NR} \to \frac{x_F}{q^2}\left[\ln\left(\frac{q^2}{\Lambda^2}\right)\right]^{-1}, \tag{37}$$

where q^2 is the invariant mass of $D^{(*)}K^{(*)}$ and $\Lambda = 0.5$ GeV is the QCD scale.

Together with the pole contribution provided in Appendix B, the complete form factors are modeled by the pole and NR contribution,

$$F(q^2) = F(q^2)|_{\rm pole} + \frac{x_F}{q^2}\left[\ln\left(\frac{q^2}{\Lambda^2}\right)\right]^{-1}, \tag{38}$$

where the asymptotic form of NR contribution is adopted for simplicity. As more data is available in the future, one could replace this simple form with a more sophisticated one to fit the data, as in Ref. [23].

III. RESULTS

A. Two-body $\mathcal{D}_s^{(*)}\bar{\mathcal{D}}_s^{(*)}$ decays and the width difference: An update

We first update the branching fractions of two-body $\bar{B}_s \to D_s^{(*)}\bar{D}_s^{(*)}$ decays, which contribute to $\Delta\Gamma_s$. The necessary parameters are given in Appendix C. Our results are listed in Table II, where experimental results and previous theoretical results from Ref. [21] are listed for comparison. Since SU(3)-related modes in $B_{u,d}$ systems are usually more precisely known than those in the B_s system, we also list them in parentheses for comparison. For example, data for $\mathcal{B}(\bar{B}_u \to D_u\bar{D}_s)$, which is approximately the same as $\mathcal{B}(\bar{B}_s \to D_s\bar{D}_s)$ under the SU(3) limit, is listed in parentheses. Note that two uncertainties are given in our results: The first uncertainty is obtained by varying decay constants and form factors by 5%, while the second comes from the estimated 10% uncertainty in a_1.

The branching fractions of $D_s^{(*)}\bar{D}_s^{(*)}$ modes are all of percent level. In general, our result is smaller than the result in Ref. [21]. These branching fractions can be compared with experimental data in both B_s and B^- systems. One can see that our results agree with experimental results within uncertainties. The direct measurement of $\bar{B}_s \to D_s^{(*)}\bar{D}_s^{(*)}$ exclusive decays was recently reported by Belle [41].[5] While the observed branching fraction of the $D_s\bar{D}_s$ mode $(1.0 \pm 0.4)\%$ is close to our result, other modes are more aligned with the calculation in Ref. [21]. But the world average of the inclusive branching fraction $\mathcal{B}(\bar{B}_s \to D_s^{(*)}\bar{D}_s^{(*)})$ [4,34] and the rates of SU(3)-related modes are closer to our results.

The total $\Delta\Gamma_f/\Gamma_s$ induced by $D_s^{(*)}\bar{D}_s^{(*)}$ modes is $10.2 \pm 2.2 \pm 2.1\%$. This value is smaller than the previous long-distance calculation [21] also shown in this table. In addition, the total $\Delta\Gamma_f/\Gamma_s$ does not reach the short-distance central value in Eq. (5). One also observes that $\Delta\Gamma_s(D_s^{(*)}\bar{D}_s^{(*)})/\Gamma_s$ is approximately 2 times the total branching fractions. The relation $|\Delta\Gamma_s(f)/\Gamma_s| \le 2\sqrt{\mathcal{B}(\bar{B}_s \to f)\mathcal{B}(B_s \to f)}$, which corresponds to the maxima in Eq. (15d), saturates only when the mode(s) f is (are) purely CP even, such as the $D_s\bar{D}_s$ mode. The nearly maximal $\Delta\Gamma_f$ reflects that $D_s^{(*)}$ are very efficient in mediating the width difference.

Several new $c\bar{s}$ resonances are found in B decays. They may also contribute to $\Delta\Gamma_s$. We calculate the contribution from the two-body modes with $D_{s0}^*(2317)$, $D_{s1}(2460)$, and $D_{s1}(2536)$. Results are shown in Table III. There are 21 additional modes when these higher D_s^{**} resonances are included. Note that not all modes are shown explicitly in

[5]Note that this measurement does not tag the flavor of the B_s meson. Although there should be a corresponding correction to the order of $\Delta\Gamma_s/\Gamma_s$ [22], it is smaller than the theoretical errors and omitted from Table II.

TABLE II. The branching fractions of $\bar{B}_s \to D_s^{(*)}\bar{D}_s^{(*)}$ decays and their contribution to the width difference. The results can be compared with data in Refs. [4,34,41]. The data for the B^- system in Ref. [34], which are related to B_s under SU(3) symmetry, are shown in parentheses (see text for details). The theoretical result of Ref. [21] is also presented for comparison.

Mode(f)	$\mathcal{B}(\bar{B}_{s,(u)} \to f)$ (%) Data	$\mathcal{B}(\bar{B}_s \to f)$ (%) This work	$\mathcal{B}(\bar{B}_s \to f)$ (%) Ref. [21]	$\Delta\Gamma_f/\Gamma_s$ (%) This work	$\Delta\Gamma_f/\Gamma_s$ (%) Ref. [21]
$D_s\bar{D}_s$	1.04 ± 0.35[a] (1.00 ± 0.17)[a]	$1.4 \pm 0.3 \pm 0.3$	1.6	$2.7 \pm 0.6 \pm 0.6$	3.1
$D_s^*\bar{D}_s + D_s\bar{D}_s^*$	2.75 ± 1.08[b] (1.58 ± 0.33)[a]	$1.8 \pm 0.4 \pm 0.4$	2.2	$3.6 \pm 0.8 \pm 0.8$	4.4
$D_s^*\bar{D}_s^*$	3.08 ± 1.49[b] (1.71 ± 0.24)[a]	$2.3 \pm 0.5 \pm 0.5$	3.6	$3.8 \pm 0.8 \pm 0.8$	6.9
$D_s^{(*)}\bar{D}_s^{(*)}$	4.9 ± 1.4[c] 6.9 ± 2.3[b] 4.0 ± 1.5[a] (4.29 ± 0.74)[a]	$5.5 \pm 1.2 \pm 1.1$	7.4	$10.2 \pm 2.2 \pm 2.1$	14.4

[a]Data taken from Ref. [34].
[b]Data taken from Ref. [41].
[c]Data taken from Ref. [4].

the Table. Since CP is conserved in this work, $\mathcal{B}(\bar{B}_s \to f) = \mathcal{B}(B_s \to \bar{f})$ and $\Delta\Gamma_f = \Delta\Gamma_{\bar{f}}$. For modes which are not CP eigenstates, the contributions from their CP conjugates are also known and should be added to $\Delta\Gamma_s/\Gamma_s$. The total branching fraction of these additional modes is comparable to the sum of $\mathcal{B}(D_s^{(*)}\bar{D}_s^{(*)})$. However, the corresponding contribution to the width difference turns out to be tiny. After considering all of these two-body modes, the total $\Delta\Gamma_f/\Gamma_s$ only increases slightly from $10.2 \pm 2.2 \pm 2.1\%$ to $10.4 \pm 2.5 \pm 2.2\%$. There are two reasons for such a tiny contribution. First, the signs of $\Delta\Gamma_f$ are fluctuating among these modes, leading to cancellations in the total sum. In addition, the mismatch effect is serious. For instance, the $\bar{B}_s \to D_s^*\bar{D}_{s1}(2460)$ mode has a

TABLE III. The branching fractions and width difference of $\bar{B}_s$ and $\bar{B}_s$ decays to two-body $D_s^{(*,**)}\bar{D}_s^{**}$, where D_s^{**} is $D_{s0}^*(2317)$, $D_{s1}(2460)$, or $D_{s1}(2536)$. We show data of SU(3)-related modes in the $\bar{B}_u$ system [34] in parentheses for comparison.

Mode(f)	$\mathcal{B}(\bar{B}_s \to f)$ (%)	$\mathcal{B}(B_s \to f)$ (%)	$\Delta\Gamma_f/\Gamma_s$ (%)
$D_s\bar{D}_{s0}^*(2317)$	$0.10 \pm 0.02 \pm 0.02$ $(0.073^{+0.022}_{-0.017})$[a]	$0.15 \pm 0.03 \pm 0.03$	$-0.24 \pm 0.05 \pm 0.05$
$D_s^*\bar{D}_{s0}^*(2317)$	$0.05 \pm 0.01 \pm 0.01$ (0.09 ± 0.07)[a]	$0.12 \pm 0.03 \pm 0.03$	$-0.15 \pm 0.03 \pm 0.03$
$D_s\bar{D}_{s1}(2460)$	$0.24 \pm 0.05 \pm 0.05$ $(0.31^{+0.10}_{-0.09})$	$0.04 \pm 0.01 \pm 0.01$	$-0.18 \pm 0.04 \pm 0.04$
$D_s^*\bar{D}_{s1}(2460)$	$0.81 \pm 0.17 \pm 0.17$ (1.20 ± 0.30)	$0.06 \pm 0.01 \pm 0.01$	$+0.16 \pm 0.03 \pm 0.03$
$D_s\bar{D}_{s1}(2536)$	$0.02 \pm 0.01 \pm 0.01$ $(0.022 \pm 0.007$[b]	$0.38 \pm 0.08 \pm 0.08$	$+0.19 \pm 0.04 \pm 0.04$
$D_s^*\bar{D}_{s1}(2536)$	$0.09 \pm 0.02 \pm 0.02$ (0.055 ± 0.0016)[b]	$0.38 \pm 0.08 \pm 0.08$	$+0.34 \pm 0.07 \pm 0.07$
$D_{s0}^*(2317)\bar{D}_{s1}(2460)$	$0.024 \pm 0.005 \pm 0.005$	$0.002 \pm 0.001 \pm 0.001$	$+0.013 \pm 0.003 \pm 0.003$
$D_{s0}^*(2317)\bar{D}_{s1}(2536)$	$0.002 \pm 0.001 \pm 0.001$	$0.017 \pm 0.004 \pm 0.004$	$-0.012 \pm 0.003 \pm 0.003$
$D_{s1}(2460)\bar{D}_{s1}(2536)$	$0.001 \pm 0.001 \pm 0.001$	$0.077 \pm 0.017 \pm 0.016$	$+0.000 \pm 0.000 \pm 0.000$
$D_{s0}^*(2317)\bar{D}_{s0}^*(2317)$	$0.009 \pm 0.002 \pm 0.002$		$+0.018 \pm 0.004 \pm 0.004$
$D_{s1}(2460)\bar{D}_{s1}(2460)$	$0.014 \pm 0.003 \pm 0.003$		$-0.010 \pm 0.002 \pm 0.002$
$D_{s1}(2536)\bar{D}_{s1}(2536)$	$0.007 \pm 0.002 \pm 0.001$		$+0.008 \pm 0.002 \pm 0.002$
Total	$2.57 \pm 0.55 \pm 0.54$		$0.24 \pm 0.27 \pm 0.05$[c]

[a]$\mathcal{B}(B^- \to D^{(*)0}\bar{D}_{s0}(2317)) \times \mathcal{B}(\bar{D}_{s0}(2317) \to \bar{D}_s\pi^-)$.
[b]$\mathcal{B}(B^- \to D^{(*)0}\bar{D}_{s1}(2536)) \times \mathcal{B}(\bar{D}_{s1}(2536) \to \bar{D}^*K^-)$.
[c]The contribution from CP-conjugate modes $\bar{f}$ is included.

TABLE IV. The branching fractions and width difference of two-body $\bar{B}_s$ and B_s decays to $D_s^{(*,**)}\bar{D}_{sJ}(2700)$, where D_s^{**} stands for $D_{s0}^*(2317)$, $D_{s1}(2460)$, or $D_{s1}(2536)$.

Mode(f)	$\mathcal{B}(\bar{B}_s \to f)$ (%)	$\mathcal{B}(B_s \to f)$ (%)	$\Delta\Gamma_f/\Gamma_s$ (%)
$D_s\bar{D}_{sJ}(2700)$	$0.44 \pm 0.18 \pm 0.09$	$0.02 \pm 0.01 \pm 0.01$	$0.21 \pm 0.08 \pm 0.04$
$D_s^*\bar{D}_{sJ}(2700)$	$2.0 \pm 0.8 \pm 0.4$	$0.08 \pm 0.03 \pm 0.02$	$0.73 \pm 0.27 \pm 0.15$
$D_s^{(*)}\bar{D}_{sJ}(2700)$	$2.5 \pm 1.0 \pm 0.5$	$0.11 \pm 0.03 \pm 0.02$	$1.9 \pm 0.7 \pm 0.4$[a]
$D_s^{**}\bar{D}_{sJ}(2700)$	$0.14 \pm 0.08 \pm 0.03$	$0.02 \pm 0.07 \pm 0.01$	$0.08 \pm 0.03 \pm 0.02$[a]

[a]The contribution from CP-conjugate modes $\bar{f}$ is included.

nonnegligible branching fraction of 0.81%, but the branching fraction of $B_s \to D_s^*\bar{D}_{s1}(2460)$ is only 0.06%. In fact, the smallness of contributions in the heavy-quark limit from p-wave resonances was expected [21], and it is confirmed in a realistic calculation given here.

The sizable branching fraction $\mathcal{B}(\bar{B} \to D^{(*)}\bar{D}_{sJ}(2700)) \times \mathcal{B}(\bar{D}_{sJ}(2700) \to \bar{D}\bar{K})$ indicates that the $\bar{D}_{sJ}(2700)$ resonance may be important for $\Delta\Gamma_s$. Since $\bar{D}_{sJ}(2700)$ has a broad width, it is expected to interfere with the continuum of $\bar{B}_s \to D_s\bar{D}^{(*)}\bar{K}$ produced by $\bar{D}_s^{(*)}$ poles (see Fig. 3 and the next subsection). For completeness, it is better to calculate the contribution of $\bar{D}_{sJ}(2700)$ to $\Delta\Gamma_s$ in three-body modes, including the on-shell and off-shell parts. However, the two-body calculation is simple and straightforward. It is, therefore, helpful to see the contribution of $\bar{D}_s^{(*,**)}D_{sJ}(2700)$ to $\Delta\Gamma_s$ first.

Using the parameters calculated in Eq. (36), the contributions from two-body modes including $\bar{D}_{sJ}(2700)$ are shown in Table IV. Several things ought to be noted: (a) The branching fractions of modes with current-produced $\bar{D}_{sJ}(2700)$ (the $\mathcal{B}(\bar{B}_s \to f)$ column of Table IV) are comparable to those of the $D_s^{(*)}\bar{D}_s^{(*)}$ modes. The two-body decays with $\bar{D}_{sJ}(2700)$ seem to be suppressed seriously by phase space at first glance. Nevertheless, this may not be true since the factorized amplitude $\langle \mathcal{D}_s^*|(V-A)_\mu|0\rangle$ [see Eq. (18)] for the current-produced meson is enhanced by mass, and the decay constant of $\bar{D}_{sJ}(2700)$ is unsuppressed. (b) For the mode $\bar{B}_s \to D_s^*\bar{D}_{sJ}(2700)$, there are several enhancement and suppression factors, when replacing D_s^* with $D_{sJ}(2700)$. First, its amplitude is dominated by s-wave and is free from additional momentum suppression. In addition, it is enhanced through the above-mentioned factorized amplitude and suppressed by phase space. The branching fraction of $\bar{B}_s \to D_s^*\bar{D}_{sJ}(2700)$ turns out to decrease $\sim$10% compared with $\bar{B}_s \to D_s^*\bar{D}_s^*$. On the contrary, the decay $\bar{B}_s \to D_s\bar{D}_{sJ}(2700)$ is p-wave. Its amplitude and thus branching fraction drop more than 50% when compared to $\bar{B}_s \to D_s\bar{D}_s^*$. The two different trends lead to a large ratio $\mathcal{B}(\bar{B}_s \to D_s^*\bar{D}_{sJ}(2700))/\mathcal{B}(\bar{B}_s \to D_s\bar{D}_{sJ}(2700)) \approx 5$. (c) The branching fractions of modes in which $\bar{D}_{sJ}(2700)$ contains the spectator quark [the $\mathcal{B}(B_s \to f)$ column] are very small. The branching fractions are suppressed not only by phase space, but also by the small transition form factors shown in Eq. (36).

The $\Delta\Gamma_s$ from $D_s^{(*)}\bar{D}_{sJ}(2700)$ is $1.9 \pm 0.7 \pm 0.4\%$. As the upper bound in Eq. (15d) implies, the $\Delta\Gamma_s/\Gamma_s$ of $\bar{D}_{sJ}(2700)$ is limited by the imbalance between the modes in which $\bar{D}_{sJ}(2700)$ is produced via current or with spectator. Nevertheless, the contribution from $D_{sJ}(2700)$ is larger than those from D_s^{**} and should not be neglected. We remark that, as we shall see in the three-body case, the transition amplitudes from $D_s^{(*)}$ poles can interfere constructively with the current-produced D_{sJ} pole and overcome the above-mentioned suppression, leading to sizable contribution to $\Delta\Gamma_s$.

B. Three-body $D_s^{(*)}\bar{D}^{(*)}\bar{K}^{(*)}$ decays and contributions to the width difference

We now turn to the three-body case. We shall first compare our results with the measured branching fractions in the $B_{u,d}$ system, starting from the pole model and including the NR effect, if necessary. After demonstrating that our calculation is consistent with data, we proceed to calculate the width difference in the B_s system.

1. Current-produced branching fractions in $B_{u,d}$ systems

Only current-produced modes with $\bar{K}$ have been measured in $\bar{B}_{u,d}$ systems. There is no measurement for the rest of the modes, including current-produced $\bar{K}^*$, and all the transition modes. A summary of current data and our results is presented in Table V. We separate the results of *BABAR* and Belle for comparison. Note that, in $\bar{B}_{u,d}$ systems, some $D^{(*)}\bar{D}^{(*)}\bar{K}^{(*)}$ modes contain both color-allowed and color-suppressed diagrams, where the latter is expected to be subleading and is neglected in this work. We have labeled these modes in the notes of the table and also add an approximation sign in front of our results. Note also that, in the calculation of $\Delta\Gamma_s$ in $\bar{B}_s$ systems, color-suppressed diagrams appear only in modes with $\eta^{(\prime)}$ and do not affect $D_s^{(*)}\bar{D}^{(*)}\bar{K}^{(*)}$ modes.

According to whether they are D or D^*, there are four types of $D^{(*)}\bar{D}^{(*)}K$ modes, which are classified into four categories as shown in Table V. Modes in each category

TABLE V. Comparison between experimental results from the *BABAR* and Belle collaborations and our results in Scenarios I (I′) and II. See text for detailed definitions.

Measurement	*BABAR* data (%)	Belle data (%)	Our results (%) Scenario I (Scenario I′) Pole model with D_{sJ} (without D_{sJ})	Scenario II Pole model + NR	Remarks
Category 1: Current-produced $\bar{D}\bar{K}$ with $\bar{B} \to D$ transition					
$\mathcal{B}(\bar{B}_u \to D_u \bar{D}_{sJ}(2700)^-) \times \mathcal{B}(\bar{D}_{sJ}(2700)^- \to \bar{D}^0 K^-)$	...	$0.113^{+0.026}_{-0.040}$[b]	$0.12 \pm 0.08 \pm 0.03$ (0)	$0.12 \pm 0.08 \pm 0.03$	Input for Scenario I
$\mathcal{B}(\bar{B}_u \to D_u \bar{D}^0 K^-)$	0.131 ± 0.014[a]	0.222 ± 0.033[b]	~ 0.23 (~ 0.07)	~ 0.11	Color-suppressed diagram neglected
$\mathcal{B}(\bar{B}_d \to D_d \bar{D}^0 K^-)$	0.107 ± 0.011[a]	...	$0.22 \pm 0.14 \pm 0.05$ ($0.06 \pm 0.03 \pm 0.01$)	$0.10^{+0.23}_{-0.02} \pm 0.02$	Input for Scenario II
$\mathcal{B}(\bar{B}_d \to D_d \bar{D}_{sJ}(2700)^-) \times \mathcal{B}(\bar{D}_{sJ}(2700)^- \to \bar{D}^0 K^-)$	...	...	$0.11 \pm 0.07 \pm 0.02$ (0)	$0.11 \pm 0.07 \pm 0.02$	
Category 2: Current-produced $\bar{D}\bar{K}$ with $\bar{B} \to D^*$ transition					
$\mathcal{B}(\bar{B}_d \to D_d^* \bar{D}^0 K^-)$	0.247 ± 0.021[a]	...	$0.67 \pm 0.45 \pm 0.14$ ($0.07 \pm 0.03 \pm 0.01$)	$0.32^{+0.75}_{-0.13} \pm 0.07$	Input for Scenario II
$\mathcal{B}(\bar{B}_d \to D_d^* \bar{D}_{sJ}(2700)^-) \times \mathcal{B}(\bar{D}_{sJ}(2700)^- \to \bar{D}^0 K^-)$	...	...	$0.50 \pm 0.33 \pm 0.11$ (0)	$0.50 \pm 0.33 \pm 0.11$	
Category 3: Current-produced $\bar{D}^*\bar{K}$ with $\bar{B} \to D$ transition					
$\mathcal{B}(\bar{B}_d \to D_d \bar{D}^{*0} K^-)$	0.346 ± 0.041[a]	...	$0.35 \pm 0.21 \pm 0.07$ ($0.20 \pm 0.10 \pm 0.04$)	$0.35 \pm 0.21 \pm 0.07$[d]	
$\mathcal{B}(\bar{B}_d \to D_d \bar{D}_{sJ}(2700)^-) \times \mathcal{B}(\bar{D}_{sJ}(2700)^- \to \bar{D}^{*0} K^-)$	...	...	$0.11 \pm 0.07 \pm 0.02$ (0)	$0.11 \pm 0.07 \pm 0.02$[d]	
Category 4: Current-produced $\bar{D}^*\bar{K}$ with $\bar{B} \to D^*$ transition					
$\mathcal{B}(\bar{B}_d \to D_d^* \bar{D}^{*0} K^-)$	1.060 ± 0.092[a]	...	$0.94 \pm 0.62 \pm 0.20$ ($0.15 \pm 0.08 \pm 0.03$)	$0.94 \pm 0.62 \pm 0.20$ [d]	
$\mathcal{B}(\bar{B}_d \to D_d^* \bar{D}_{sJ}(2700)^-) \times \mathcal{B}(\bar{D}_{sJ}(2700)^- \to D^{*0} K^-)$	...	...	$0.52 \pm 0.33 \pm 0.11$ (0)	$0.52 \pm 0.33 \pm 0.11$[d]	
$\mathcal{B}(\bar{B}_d \to D_d^* \bar{D}^{*+} \bar{K}^0)$	0.826 ± 0.080[a]	...	~ 0.91 (~ 0.15)	~ 0.91[d]	Color-suppressed diagram neglected
$\mathcal{B}(\bar{B}_d \to D_d^* \bar{D}^{*+} K_S^0)$	0.44 ± 0.08[c]	0.34 ± 0.08[c]	~ 0.46 (~ 0.07)	~ 0.46[d]	Color-suppressed diagram neglected

[a]Data taken from Ref. [28].
[b]Data taken from Ref. [26].
[c]Data taken from Ref. [25].
[d]In Scenario II, the results of modes in Categories 3 and 4 are the same as for Scenario I.

have similar branching fractions because of SU(2) symmetry. The measured branching fractions increase from Category 1 ($\sim 0.1\%$) to Category 4 ($\sim 1\%$). One can find tension in measurements of $\bar{B}_u \to D_u \bar{D}^0 K^-$. A large $\bar{D}_{sJ}(2700)$ contribution has been observed in $\bar{B}_u \to D_u \bar{D}^0 K^-$ by Belle only [26], but in 2.2σ disagreement with *BABAR* [28]. The tension in data becomes more severe if one compares the $\bar{D}_{sJ}(2700)$ contribution to the total branching fraction of $\bar{B}_u \to D_u \bar{D}^0 K^-$. In the case of Belle, the contribution from $\bar{D}_{sJ}(2700)$ is about half the total branching fraction. However, it is approximately equal to the total branching fraction for *BABAR*. As we show, the inconsistency makes it difficult to explain all data with a simple pole model.

The results of our calculation in different scenarios are compared with experiments in Table V. In Scenario I, $D_s^{(*)}$ and D_{sJ} poles are used, while in Scenario I′, only $D_s^{(*)}$ poles are considered, with results shown in parentheses for comparison. In Scenario II, NR contributions in $\bar{D}\bar{K}$ timelike form factors are included to demonstrate that the inconsistency with experiments in Scenario I can be resolved. Note that no NR contribution is introduced for modes in Categories 3 and 4, as the pole model results (Scenario I) already agree with the data. Furthermore, as there are no measurements on transition modes and modes with $\bar{K}^*$, no NR contribution is applied to these modes. The two uncertainties of our results are obtained by the same method as in two-body case, but with additional uncertainties from strong couplings included in the first errors.

Despite the disagreement between data, we first attempt to explain all measurements only with a pole model (Scenario I). The corresponding diagrams can be found in the left portion of Fig. 3 with the appropriate spectator quark. In the calculation, we first fix the decay constant of $D_{sJ}(2700)$ from the contribution of $\bar{D}_{sJ}(2700)$ in the $\bar{B}_u \to D_u \bar{D}^0 K^-$ decay. The value of this decay constant was shown in Eq. (36), and the value agrees with those obtained in other studies (see Sec. II D). The total branching fraction of $\bar{B}_u \to D_u \bar{D}^0 K^-$ is consistent with Belle's measurement, and inevitably less consistent with the *BABAR* result and the SU(2)-related mode $\bar{B}_d \to D_d \bar{D}^0 K^-$. Unfortunately, there is no measurement on the $\bar{B}_d \to D_d \bar{D}^0 K^-$ rate from Belle yet. For Category 2, the total branching fraction $\bar{B}_d \to D_d^* \bar{D}^0 K^-$ is about 2.5 times larger than the *BABAR* result, as in Category 1. Again, there is no measurement from Belle. More data analysis is called for. Nevertheless, it is interesting to see that our predicted results on branching fractions in Categories 3 and 4 agree well with data.

To explain the total branching fractions in Scenario I, we must start from the $\bar{D}_{sJ}(2700)$ contribution, which has on-shell as well as off-shell parts. Roughly speaking, the $\bar{D}_{sJ}(2700)$ contribution can be understood by using the narrow width approximation. The contribution in Category 1 (2) is almost the same as in Category 3 (4). This is expected since the two categories are different from each other only in $\bar{D}_{sJ}(2700) \to \bar{D}^* \bar{K}$, $\bar{D}\bar{K}$ parts, which have nearly the same branching fractions [see Eq. (33)]. The contribution in Category 2 is about 5 times larger than in Category 1, where the $\bar{B} \to D^*$ transition is replaced with $\bar{B} \to D$. This factor already appeared in the two-body branching fractions of $\bar{B}_s \to D_s^{(*)} \bar{D}_{sJ}$ modes shown in Table IV. However, a closer look reveals that the precise $D_{sJ}(2700)$ contribution should be obtained by integrating the full three-body phase space, as the width of $D_{sJ}(2700)$ is of the order of 0.1 GeV, which is not narrow enough compared with the three-body phase space. (For instance, in the decay of $\bar{B}_s \to D_s^* \bar{D}_{sJ}(2700)$ with $\bar{D}_{sJ}(2700) \to \bar{D}^* \bar{K}$, the invariant mass of $\bar{D}^* \bar{K}$ ranges roughly from 2.5 GeV to 3.3 GeV. The Breit-Wigner function for $D_{sJ}(2700)$, with a peak at 2.7 GeV, cannot be approximated as a delta function since its peak is less than 2 times the width above the lower limit of the invariant mass of $\bar{D}^{(*)} \bar{K}$.) The numerical results usually show a 10% overestimation by narrow width approximation. In addition, the $\bar{D}_{sJ}(2700)$ contribution in $\bar{B}_d \to D_d^* \bar{D}^{*0} K^-$ is slightly greater than $\bar{B}_d \to D_d^* \bar{D}^0 K^-$, whereas the ratio in Eq. (33) is the other way around. This is due to the contribution from the off-shell part. The off-shell contribution in the high-momentum region favors $\bar{D}_{sJ}(2700) \to \bar{D}^* \bar{K}$ over $\bar{D}_{sJ}(2700) \to \bar{D}\bar{K}$, as one can see from the strong interaction matrix elements in Eq. (31). The former coupling is quadratic in momentum, while the latter is only linear. The numerical results show that the off-shell effect is about 10%. This correction also echoes our assertion that the contribution of $D_{sJ}(2700)$ should be treated in a three-body picture.

The effect of off-shell $\bar{D}_s^{(*)}$ poles can be read from Scenario I′ shown in parentheses in Table V. For the first two categories, only the $\bar{D}_s^*$ pole contributes, while for the latter two categories, containing the current-generated $\bar{D}^* \bar{K}$, the $\bar{D}_s$ pole starts to contribute as well. This explains why modes in Categories 3 and 4 have larger branching fractions in Scenario I′. It is interesting to note that all branching fractions in Scenario I′ are deficient in explaining experimental results. The $D_{sJ}(2700)$ resonance provides an important source for the nonnegligible three-body branching fractions of current-produced modes. Comparing with Scenario I, one finds the interference between $D_{sJ}(2700)$ and $D_s^{(*)}$ poles is not negligible. For example, in the $\bar{B}^0 \to D^{*+} \bar{D}^{*0} K^-$ decay rate (see Category 4 in Table V), the $\bar{D}_s^{(*)}$ and $\bar{D}_{sJ}$ contributions are $\sim 0.15\%$ and $\sim 0.52\%$, respectively, while the total predicted rate is $\sim 0.94\%$, which implies a fairly effective constructive interference between these poles. If the D_{sJ} width were narrow, we would expect the interference effect to be negligible and it would be enough to consider a real $D_{sJ}(2700)$ in two-body final states.

After the above discussion, one can now understand the total branching fractions in Scenario I by combining

contributions of three different poles (see the left portion of Fig. 3). The contribution of $\bar{D}_{sJ}(2700)$ dominates over $\bar{D}_s^{(*)}$. To first order, Category 2 ($D^*\bar{D}\bar{K}$) and Category 4 ($D^*\bar{D}^*\bar{K}$) have the same branching fractions from $\bar{D}_{sJ}(2700)$ and are larger than Category 1 ($D\bar{D}\bar{K}$) and Category 3 ($D\bar{D}^*\bar{K}$). $\bar{D}_s^{(*)}$ poles further split the two categories that have almost the same $\bar{D}_{sJ}(2700)$ contribution. Consequently, modes in Category 4 ($D^*\bar{D}^*\bar{K}$) have larger total branching fractions than those in Category 2 ($D^*\bar{D}\bar{K}$), and similarly for Category 3 ($D\bar{D}^*\bar{K}$) and 1 ($D\bar{D}\bar{K}$). The three different poles form the hierarchy of total branching fractions of the four categories in Scenario I.

Now we consider the situation in which both the measurements of *BABAR* and the contribution of $D_{sJ}(2700)$ measured by Belle are confirmed in the future. We demonstrate that it is possible to reproduce almost all measurements by using Scenario II: a pole model with NR contribution in timelike form factors of $\bar{D}\bar{K}$, in addition. Note that the first two categories share the same current-produced $\bar{D}\bar{K}$, while $\bar{D}^*\bar{K}$ form factors appear only in Categories 3 and 4. Since modes in the last two categories already agree with data in Scenario I, using pole model only, no NR contribution is introduced in $\bar{D}^*\bar{K}$ form factors. The branching fractions of modes in the first two categories can be tuned by two complex NR parameters in the timelike form factors of $\bar{D}\bar{K}$. These two parameters are fixed by fitting to the observed branching fractions of $\bar{B}_d \to D_d\bar{D}^0K^-$ and $\bar{B}_d \to D_d^*\bar{D}^0K^-$ (denoted in the notes in Table V). The best fit gives $x_{F_0}^{DK} = (-75 + 52i)$ GeV^2 and $x_{F_1}^{DK} = (16 + 2i)$ GeV^2, where $x_{F_0}^{DK}$ and $x_{F_1}^{DK}$ correspond to the NR contribution in $\bar{D}\bar{K}$ timelike form factors F_0 and F_1, respectively [see Eq. (38)]. Usually the two complex (four real) NR parameters cannot be fully determined from two constraints. In this case, however, there is a localized and huge $D_{sJ}(2700)$ resonance contribution in the $\bar{B}_d \to D_d^*\bar{D}^0K^-$ mode. The NR contribution, which is smooth in phase space, has to cancel the $D_{sJ}(2700)$ contribution while maintaining the form factors in other parts of phase space. In other words, the phases of the NR parameters are constrained by the complex resonance, while the magnitudes, which control NR parts in the off-resonance region, are limited by data. The branching fractions of the fit are shown in Table V, where 100% uncertainties in x's are included in the first errors. In this scenario, all experimental results, except for the explicit disagreement in $\bar{B}_u \to D_u\bar{D}^0K^-$ between data, can be explained within uncertainty when NR is included. In particular, the $\bar{B}_d \to D_d^*\bar{D}^0K^-$ rate is now reduced by a factor of 2 and consistent with data within errors.

2. Branching fractions in the B_s system and the width difference

After checking the validity of our calculations by comparing them to existing data on rates, we move to our main purpose: estimating $\Delta\Gamma_s$. The relevant diagram is shown in Fig. 3. In Table VI, we show our results in Scenarios I (I′). Recall that bounds on $\Delta\Gamma_s$ are related to rates [see Eq. (15d)]. The branching fractions of current-produced modes and transition modes are also shown, and can be read from $\mathcal{B}_{\mathcal{J}}(\bar{B}_s \to f)$ and $\mathcal{B}_{\mathcal{T}}(B_s \to f)$, respectively. For simplicity, only modes with $\bar{K}^{(*)}$ are shown; the results of modes with $K^{(*)}$ can be derived from their CP conjugates. As noted before, since CP is conserved in this work, $\mathcal{B}(\bar{B}_s \to f) = \mathcal{B}(B_s \to \bar{f})$ and $\Delta\Gamma_f = \Delta\Gamma_{\bar{f}}$. The total $\Delta\Gamma_f/\Gamma_s$ contains the modes in the table and their CP conjugates, so it is twice the sum of the listed $\Delta\Gamma_f/\Gamma_s$ in the table.

Before discussing $\Delta\Gamma_s$, we first look at the branching fractions of these modes. Current-produced modes in $\bar{B}_s$ decays are SU(3)-related to modes considered previously. Their rates are similar. For example, $\bar{B}_s \to D_s^*\bar{D}^*K$ modes have the largest rates ($\sim 0.88\%$) as the $\bar{B}_{u,d} \to D_{u,d}^*\bar{D}^*K$ modes. However, the transition modes are new. Their rates are subpercent or smaller. Note that, while current-produced modes with $\bar{K}$ are dominated by $D_{sJ}(2700)$, transition modes do not change significantly when $\bar{D}_{sJ}(2700)$ is included. For instance, without $\bar{D}_{sJ}$, the branching fraction of current-produced mode $\bar{B}_s \to D_s^*\bar{D}^0K^-$ drops from 0.64% to 0.07%. In contrast, it drops only from 0.09% to 0.06% for the branching fraction of transition mode $B_s \to D_s^*\bar{D}^0K^-$. The distinct behavior is not surprising because the $B_s \to D_s^*\bar{D}_{sJ}(2700)$ rate (before $\bar{D}_{sJ} \to \bar{D}^0K^-$) is relatively suppressed compared to the $B_s \to D_s^*\bar{D}_s^*$ ones (before $\bar{D}_s^* \to \bar{D}^0K^-$) (see Sec. III A). As we will see later, the different roles played by these poles will be useful for enhancing $\Delta\Gamma_s$ through interferences.

As the branching fractions of transition modes are not tiny, one would expect a nonnegligible $\Delta\Gamma_s$. The $\Delta\Gamma_f/\Gamma_s$ of three-body modes range from 0.07% to 0.65%, as shown in Table VI. The last two modes with $\bar{K}$ have the largest $\Delta\Gamma_f$, as their rates are largest. In this scenario, the total $\Delta\Gamma_s/\Gamma_s$ is

$$\begin{aligned}
\Delta\Gamma_s/\Gamma_s(D_s^{(*,**)}\bar{D}_s^{(*,**)}) &= (10.4 \pm 2.5 \pm 2.2)\%,\\
\Delta\Gamma_s/\Gamma_s(D_s^{(*)}\bar{D}^{(*)}\bar{K} + \bar{D}_s^{(*)}D^{(*)}K) &= (5.9 \pm 3.6 \pm 1.2)\%,\\
\Delta\Gamma_s/\Gamma_s(D_s^{(*)}\bar{D}^{(*)}\bar{K}^* + \bar{D}_s^{(*)}D^{(*)}K^*) &= (1.9 \pm 0.9 \pm 0.4)\%,\\
\Delta\Gamma_s/\Gamma_s &= (18.2 \pm 7.0 \pm 3.8)\%.
\end{aligned} \tag{39}$$

Clearly, the $\Delta\Gamma_s$ of three-body modes is comparable to two-body modes. The $\Delta\Gamma_s$ of three-body modes is composed mainly of modes with K. It shows that the approximation in which $D_s^{(*)}\bar{D}_s^{(*)}$ modes saturate $\Delta\Gamma_s$ is dubious. In addition, Eq. (39) agrees with the short-distance calculation in Eq. (5) within uncertainties. There is no evidence of

TABLE VI. The branching fractions ($\mathcal{B}_{\mathcal{J},\mathcal{T}}$) and width difference ($\Delta\Gamma_f$) of the three-body $D_s^{(*)}\bar{D}^{(*)}\bar{K}^{(*)}$ modes in the scenario with only pole contribution. $\mathcal{B}_{\mathcal{J}}$ and $\mathcal{B}_{\mathcal{T}}$ denote the current-produced decay ($\bar{B}_s \to f$) and the transitional decay ($B_s \to f$), respectively. $D_{sJ}(2700)$ is not included in modes with $\bar{K}^*$ in this scenario. The results with only $D_s^{(*)}$ poles are shown in parentheses.

Scenario I (I′) Pole Contribution Only							
Modes with $\bar{K}$				Modes with $\bar{K}^*$			
Mode(f)	$\mathcal{B}_{\mathcal{J}}(\bar{B}_s \to f)$ (%)	$\mathcal{B}_{\mathcal{T}}(B_s \to f)$ (%)	$\Delta\Gamma_f/\Gamma_s$ (%)	Mode(f)	$\mathcal{B}_{\mathcal{J}}(\bar{B}_s \to f)$ (%)	$\mathcal{B}_{\mathcal{T}}(B_s \to f)$ (%)	$\Delta\Gamma_f/\Gamma_s$ (%)
$D_s\bar{D}^0K^-$	$0.19 \pm 0.12 \pm 0.04$	$0.04 \pm 0.02 \pm 0.01$	$0.17 \pm 0.10 \pm 0.03$	$D_s\bar{D}^0K^{*-}$	$(0.07 \pm 0.03 \pm 0.01)$	$(0.03 \pm 0.01 \pm 0.01)$	$(0.08 \pm 0.04 \pm 0.02)$
	$(0.06 \pm 0.03 \pm 0.01)$	$(0.03 \pm 0.02 \pm 0.01)$	$(0.09 \pm 0.04 \pm 0.02)$				
$D_sD^-\bar{K}^0$	$0.19 \pm 0.12 \pm 0.04$	$0.04 \pm 0.02 \pm 0.01$	$0.16 \pm 0.09 \pm 0.03$	$D_sD^-\bar{K}^{*0}$	$(0.06 \pm 0.03 \pm 0.01)$	$(0.03 \pm 0.01 \pm 0.01)$	$(0.08 \pm 0.04 \pm 0.02)$
	$(0.05 \pm 0.03 \pm 0.01)$	$(0.03 \pm 0.02 \pm 0.01)$	$(0.08 \pm 0.04 \pm 0.02)$				
$D_s^*\bar{D}^0K^-$	$0.64 \pm 0.43 \pm 0.13$	$0.09 \pm 0.05 \pm 0.02$	$0.38 \pm 0.23 \pm 0.08$	$D_s^*\bar{D}^0K^{*-}$	$(0.04 \pm 0.02 \pm 0.01)$	$(0.03 \pm 0.02 \pm 0.01)$	$(0.07 \pm 0.03 \pm 0.01)$
	$(0.07 \pm 0.03 \pm 0.01)$	$(0.06 \pm 0.03 \pm 0.01)$	$(0.12 \pm 0.05 \pm 0.03)$				
$D_s^*D^-\bar{K}^0$	$0.62 \pm 0.42 \pm 0.13$	$0.09 \pm 0.05 \pm 0.02$	$0.37 \pm 0.22 \pm 0.08$	$D_s^*D^-\bar{K}^{*0}$	$(0.04 \pm 0.02 \pm 0.01)$	$(0.03 \pm 0.02 \pm 0.01)$	$(0.07 \pm 0.03 \pm 0.02)$
	$(0.07 \pm 0.03 \pm 0.01)$	$(0.06 \pm 0.03 \pm 0.01)$	$(0.11 \pm 0.05 \pm 0.02)$				
$D_s\bar{D}^{*0}K^-$	$0.30 \pm 0.18 \pm 0.06$	$0.09 \pm 0.05 \pm 0.02$	$0.31 \pm 0.21 \pm 0.06$	$D_s\bar{D}^{*0}K^{*-}$	$(0.18 \pm 0.08 \pm 0.04)$	$(0.08 \pm 0.04 \pm 0.02)$	$(0.24 \pm 0.12 \pm 0.05)$
	$(0.17 \pm 0.08 \pm 0.04)$	$(0.08 \pm 0.04 \pm 0.02)$	$(0.23 \pm 0.11 \pm 0.05)$				
$D_sD^{*-}\bar{K}^0$	$0.29 \pm 0.18 \pm 0.06$	$0.09 \pm 0.04 \pm 0.02$	$0.30 \pm 0.20 \pm 0.06$	$D_sD^{*-}\bar{K}^{*0}$	$(0.17 \pm 0.08 \pm 0.04)$	$(0.08 \pm 0.04 \pm 0.02)$	$(0.24 \pm 0.11 \pm 0.05)$
	$(0.17 \pm 0.08 \pm 0.04)$	$(0.08 \pm 0.04 \pm 0.02)$	$(0.22 \pm 0.11 \pm 0.05)$				
$D_s^*\bar{D}^{*0}K^-$	$0.89 \pm 0.59 \pm 0.18$	$0.17 \pm 0.09 \pm 0.03$	$0.65 \pm 0.39 \pm 0.14$	$D_s^*\bar{D}^{*0}K^{*-}$	$(0.05 \pm 0.02 \pm 0.01)$	$(0.04 \pm 0.02 \pm 0.01)$	$(0.08 \pm 0.04 \pm 0.02)$
	$(0.14 \pm 0.07 \pm 0.03)$	$(0.11 \pm 0.05 \pm 0.02)$	$(0.23 \pm 0.11 \pm 0.05)$				
$D_s^*D^{*-}\bar{K}^0$	$0.86 \pm 0.57 \pm 0.18$	$0.16 \pm 0.09 \pm 0.03$	$0.64 \pm 0.38 \pm 0.13$	$D_s^*D^{*-}\bar{K}^{*0}$	$(0.05 \pm 0.02 \pm 0.01)$	$(0.03 \pm 0.02 \pm 0.01)$	$(0.08 \pm 0.04 \pm 0.02)$
	$(0.14 \pm 0.06 \pm 0.03)$	$(0.10 \pm 0.05 \pm 0.02)$	$(0.22 \pm 0.10 \pm 0.05)$				
Total			$5.9 \pm 3.6 \pm 1.2$[a]	Total			$(1.9 \pm 0.9 \pm 0.4)$[a]
			$(2.6 \pm 1.2 \pm 0.5)$[a]				

[a]The contribution from *CP* conjugate modes is included.

violation of the short-distance result and the underlying OPE assumption.

The interference between $\bar{D}_{sJ}(2700)$ and $\bar{D}_s^{(*)}$ can be studied by comparing Scenario I with Scenario I′ and the result of $\bar{D}_{sJ}(2700)$. The full treatment of modes with $\bar{K}$ in Scenario I, where $\bar{D}_{sJ}(2700)$ and $\bar{D}_s^{(*)}$ are taken into consideration simultaneously, gives $\Delta\Gamma_s/\Gamma_s \simeq 5.9\%$. On the other hand, one can treat $\bar{D}_{sJ}(2700)$ and $\bar{D}_s^{(*)}$ separately and sum their $\Delta\Gamma_s/\Gamma_s$. The contribution of $\bar{D}_s^{(*)}$ only (Scenario I′) can be read from Table VI. For $\bar{D}_{sJ}(2700)$, its contribution can be estimated from the two-body calculation (see Sec. III A) with the narrow width approximation. We further check that it decreases from the two-body result of 1.9% to 1.7%, when the full three-body calculation is imposed. In the case that $\bar{D}_{sJ}(2700)$ and $\bar{D}_s^{(*)}$ are summed separately, the total $\Delta\Gamma_s/\Gamma_s$ of modes with $\bar{K}$ is only $2.6\% + 1.7\% = 4.3\%$, smaller than the 5.9% in Scenario 1. The difference, which is about the size of the $\bar{D}_{sJ}$ contribution alone, shows that there is considerable interference between $\bar{D}_{sJ}(2700)$ and $\bar{D}_s^{(*)}$ poles. Such interference can be understood as follows. As depicted in Fig. 3, the $\bar{D}^{(*)}\bar{K}^{(*)}$ pairs emitted by the current-produced $\bar{D}_{sJ}(2700)$ pole interfere with the same states from the transited $\bar{D}_s^{(*)}$ poles in the transition side of the diagram. Unlike the highly suppressed $B_s \to \bar{D}_{sJ}$ transitions (see Table IV), the $B_s \to \bar{D}_s^{(*)}$ transitions are sizable (see Table II), leading to enhanced $\bar{B}_s - B_s$ mixing and $\Delta\Gamma_s$. In short, $\Delta\Gamma_s$ receives the interference contributions from the current-produced $\bar{D}_{sJ}(2700)$ pole (from $\bar{B}_s$ decays) and the transited $\bar{D}_s^{(*)}$ poles (from B_s decays), which bypass the mismatch of current-produced and transited $\bar{D}_{sJ}$ in two-body modes. In total, diagrams containing $\bar{D}_{sJ}$ poles contribute more than those with $\bar{D}_s^{(*)}$ poles only.

One can bound the width difference in Table VI by Eq. (15d). For example, the $\Delta\Gamma_f/\Gamma_s$ is bounded to be 0.77% and 0.08% for $D_s^*\bar{D}^{*0}K^-$ and $D_s^*\bar{D}^{*0}K^{*-}$ modes, respectively. Comparing to $\Delta\Gamma_f$, we see that the bounds in modes with $\bar{K}$ are higher within 20%, while they constrain $\Delta\Gamma_f$ very well for modes with $\bar{K}^*$. The accuracy of $\Delta\Gamma_f$ estimation in modes with $\bar{K}^*$ has to do with the virtual $\bar{D}_s^{(*)}$ poles. The pole contribution of $\bar{D}_s^{(*)}$ is almost real and so are the resulting amplitudes. As a result, the suppression from the inequality of Eq. (15b) is tiny for modes with $\bar{K}^*$. This demonstrates that the virtual $\bar{D}_s^{(*)}$ poles are very efficient for mediating the width difference. On the contrary, the on-shell $\bar{D}_{sJ}(2700)$, which plays an important role in modes with $\bar{K}$, generates complex amplitudes and result in the suppression of $\Delta\Gamma_f$ in these modes.

The results of Scenario II are shown in Table VII. Only the first four modes with $\bar{K}$ are different from Scenario I. Note that all transition modes and modes with $\bar{K}^*$ are still the same as in Scenario I, since there is no measurement at all to call for other contribution beyond the pole model. One can read from the table that the $\Delta\Gamma_f$ of the first four modes (modes with NR) drop by 50% to 70%. The decrease is caused by the reduction of the branching fractions in current-produced modes. Moreover, the actual $\Delta\Gamma_f$ moves away from the upper bound in Eq. (15d) when the complex NR contributions are included. In this scenario, the total $\Delta\Gamma_s/\Gamma_s$ is

$$\begin{aligned}
\Delta\Gamma_s/\Gamma_s(D_s^{(*,**)}\bar{D}_s^{(*,**)}) &= (10.4 \pm 2.5 \pm 2.2)\%, \\
\Delta\Gamma_s/\Gamma_s(D_s^{(*)}\bar{D}^{(*)}\bar{K} + \bar{D}_s^{(*)}D^{(*)}K) &= (4.5 \pm 4.4 \pm 0.9)\%, \\
\Delta\Gamma_s/\Gamma_s(D_s^{(*)}\bar{D}^{(*)}\bar{K}^* + \bar{D}_s^{(*)}D^{(*)}K^*) &= (1.9 \pm 0.9 \pm 0.4)\%, \\
\Delta\Gamma_s/\Gamma_s &= (16.7 \pm 7.8 \pm 3.5)\%.
\end{aligned} \tag{40}$$

Despite the drop of $\Delta\Gamma_f$ in modes with NR, the total $\Delta\Gamma_s$ remains similar to Scenario I because these modes are not dominant in $\Delta\Gamma_s$. Most features are similar to the previous case. The effect of three-body modes is still nonnegligible. It is interesting to see that the central value is more consistent with the short-distance calculation. The conclusion remains the same as in Scenario I.

IV. DISCUSSION

We have seen that $\bar{D}_{sJ}(2700)$ is important in modes with $\bar{K}$. One expects $\bar{D}_{sJ}(2700)$ to be nonnegligible in modes with $\bar{K}^*$ as well. Even though $\bar{D}_{sJ}(2700)$ is not heavy enough to decay to on-shell $\bar{D}^{(*)}\bar{K}^*$, its width is wide and its mass is close to the invariant mass threshold of $\bar{D}^{(*)}\bar{K}^*$. Unfortunately, there is no information about the coupling constants of the effective Lagrangian for $\bar{D}_{sJ}(2700) \to \bar{D}^{(*)}\bar{K}^*$. Unlike the on-shell $\bar{D}_{sJ}(2700) \to \bar{D}^{(*)}\bar{K}$ decay, we cannot extract the coupling constant of $\bar{D}_{sJ}(2700) \to \bar{D}^{(*)}\bar{K}^*$ directly from data. Thus, for illustration, we set the coupling constants in analogy to the coupling constants of $\bar{D}^*$ to $\bar{D}^{(*)}\bar{K}^{(*)}$ vertices

$$\tilde{g}_{D_{sJ}D^{(*)}K^*} \approx \tilde{g}_{D_{sJ}D^{(*)}K}\left(\frac{g_{D^*D^{(*)}K^*}}{g_{D^*D^{(*)}K}}\right) \approx 0.5 \times \tilde{g}_{D_{sJ}D^{(*)}K}. \tag{41}$$

Table VIII shows the result in this analogy, which we call Scenario III. The results of modes with $\bar{K}$ remain the same as in Scenario II.

Comparing with the results in previous scenarios, all branching fractions and $\Delta\Gamma_f$ increase. As before, the effect of $\bar{D}_{sJ}(2700)$ is stronger in current-produced modes than in transition modes. In particular, current-produced modes in Categories 2 ($D_s^*\bar{D}\bar{K}^*$) and 4 ($D_s^*\bar{D}^*\bar{K}^*$) are very sensitive to the appearance of $\bar{D}_{sJ}(2700)$. Their branching fractions rise at least 4 times. This large effect of current-produced $D_{sJ}(2700)$ in Categories 2 and 4 is similar to

TABLE VII. The branching fractions ($\mathcal{B}_{\mathcal{J},\mathcal{T}}$) and width difference ($\Delta\Gamma_f$) of the three-body $D_s^{(*)}\bar{D}^{(*)}\bar{K}^{(*)}$ modes in Scenario II where $\bar{D}\,\bar{K}$ timelike form factors have NR contribution. The notation is the same as in Table VI.

Scenario II Pole contribution + NR in $\bar{D}\,\bar{K}$ timelike form factors							
Modes with $\bar{K}$				Modes with $\bar{K}^*$			
Mode(f)	$\mathcal{B}_{\mathcal{J}}(\bar{B}_s \to f)$ (%)	$\mathcal{B}_{\mathcal{T}}(B_s \to f)$ (%)	$\Delta\Gamma_f/\Gamma_s$ (%)	Mode(f)	$\mathcal{B}_{\mathcal{J}}(\bar{B}_s \to f)$ (%)	$\mathcal{B}_{\mathcal{T}}(B_s \to f)$ (%)	$\Delta\Gamma_f/\Gamma_s$ (%)
$D_s\bar{D}^0K^-$	$0.09^{+0.22}_{-0.02} \pm 0.02$	$0.04 \pm 0.02 \pm 0.01$	$0.08 \pm 0.15 \pm 0.01$	$D_s\bar{D}^0K^{*-}$	$(0.07 \pm 0.03 \pm 0.01)$	$(0.03 \pm 0.01 \pm 0.01)$	$(0.08 \pm 0.04 \pm 0.02)$
$D_sD^-\bar{K}^0$	$0.09^{+0.22}_{-0.02} \pm 0.02$	$0.04 \pm 0.02 \pm 0.01$	$0.07 \pm 0.13 \pm 0.01$	$D_sD^-\bar{K}^{*0}$	$(0.06 \pm 0.03 \pm 0.01)$	$(0.03 \pm 0.01 \pm 0.01)$	$(0.08 \pm 0.04 \pm 0.02)$
$D_s^*\bar{D}^0K^-$	$0.31^{+0.74}_{-0.13} \pm 0.13$	$0.09 \pm 0.05 \pm 0.02$	$0.11 \pm 0.38 \pm 0.02$	$D_s^*\bar{D}^0K^{*-}$	$(0.04 \pm 0.02 \pm 0.01)$	$(0.03 \pm 0.02 \pm 0.01)$	$(0.07 \pm 0.03 \pm 0.01)$
$D_s^*D^-\bar{K}^0$	$0.29^{+0.71}_{-0.13} \pm 0.13$	$0.09 \pm 0.05 \pm 0.02$	$0.11 \pm 0.38 \pm 0.02$	$D_s^*D^-\bar{K}^{*0}$	$(0.04 \pm 0.02 \pm 0.01)$	$(0.03 \pm 0.02 \pm 0.01)$	$(0.07 \pm 0.03 \pm 0.02)$
$D_s\bar{D}^{*0}K^-$	$0.30 \pm 0.18 \pm 0.06$	$0.09 \pm 0.05 \pm 0.02$	$0.31 \pm 0.21 \pm 0.06$	$D_s\bar{D}^{*0}K^{*-}$	$(0.18 \pm 0.08 \pm 0.04)$	$(0.08 \pm 0.04 \pm 0.02)$	$(0.24 \pm 0.12 \pm 0.05)$
$D_sD^{*-}\bar{K}^0$	$0.29 \pm 0.18 \pm 0.06$	$0.09 \pm 0.04 \pm 0.02$	$0.30 \pm 0.20 \pm 0.06$	$D_sD^{*-}\bar{K}^{*0}$	$(0.17 \pm 0.08 \pm 0.04)$	$(0.08 \pm 0.04 \pm 0.02)$	$(0.24 \pm 0.11 \pm 0.05)$
$D_s^*\bar{D}^{*0}K^-$	$0.89 \pm 0.59 \pm 0.18$	$0.17 \pm 0.09 \pm 0.03$	$0.65 \pm 0.39 \pm 0.14$	$D_s^*\bar{D}^{*0}K^{*-}$	$(0.05 \pm 0.02 \pm 0.01)$	$(0.04 \pm 0.02 \pm 0.01)$	$(0.08 \pm 0.04 \pm 0.02)$
$D_s^*D^{*-}\bar{K}^0$	$0.86 \pm 0.57 \pm 0.18$	$0.16 \pm 0.09 \pm 0.03$	$0.64 \pm 0.38 \pm 0.13$	$D_s^*D^{*-}\bar{K}^{*0}$	$(0.05 \pm 0.02 \pm 0.01)$	$(0.03 \pm 0.02 \pm 0.01)$	$(0.08 \pm 0.04 \pm 0.02)$
Total			$4.5 \pm 4.4 \pm 0.9$[a]	Total			$(1.9 \pm 0.9 \pm 0.4)$[a]

[a]The contribution from *CP* conjugate modes is included.

TABLE VIII. The branching fractions ($\mathcal{B}_{\mathcal{J},\mathcal{T}}$) and width difference ($\Delta\Gamma_f$) of the three-body $D_s^{(*)}\bar{D}^{(*)}\bar{K}^{(*)}$ modes in Scenario III, where $D_{sJ}(2700)$ is included in all modes. The notation is the same as in Table VI.

Scenario III $D_{sJ}(2700)$ is included in all modes							
Modes with $\bar{K}$				Modes with $\bar{K}^*$			
Mode(f)	$\mathcal{B}_{\mathcal{J}}(\bar{B}_s \to f)$ (%) (exp.)	$\mathcal{B}_{\mathcal{T}}(B_s \to f)$ (%)	$\Delta\Gamma_f/\Gamma_s$ (%) (limit)	Mode(f)	$\mathcal{B}_{\mathcal{J}}(\bar{B}_s \to f)$ (%)	$\mathcal{B}_{\mathcal{T}}(B_s \to f)$ (%)	$\Delta\Gamma_f/\Gamma_s$ (%) (limit)
$D_s\bar{D}^0K^-$	$0.09^{+0.22}_{-0.02} \pm 0.02$	$0.04 \pm 0.02 \pm 0.01$	$0.08 \pm 0.15 \pm 0.01$	$D_s\bar{D}^0K^{*-}$	$0.10 \pm 0.05 \pm 0.02$	$0.03 \pm 0.02 \pm 0.01$	$0.11 \pm 0.05 \pm 0.02$
$D_sD^-\bar{K}^0$	$0.09^{+0.22}_{-0.02} \pm 0.02$	$0.04 \pm 0.02 \pm 0.01$	$0.07 \pm 0.13 \pm 0.01$	$D_sD^-\bar{K}^{*0}$	$0.09 \pm 0.05 \pm 0.02$	$0.03 \pm 0.01 \pm 0.01$	$0.10 \pm 0.05 \pm 0.02$
$D_s^*\bar{D}^0K^-$	$0.31^{+0.74}_{-0.13} \pm 0.13$	$0.09 \pm 0.05 \pm 0.02$	$0.11 \pm 0.38 \pm 0.02$	$D_s^*\bar{D}^0K^{*-}$	$0.27 \pm 0.13 \pm 0.06$	$0.06 \pm 0.03 \pm 0.01$	$0.23 \pm 0.11 \pm 0.05$
$D_s^*D^-\bar{K}^0$	$0.29^{+0.71}_{-0.13} \pm 0.13$	$0.09 \pm 0.05 \pm 0.02$	$0.11 \pm 0.38 \pm 0.02$	$D_s^*D^-\bar{K}^{*0}$	$0.25 \pm 0.12 \pm 0.06$	$0.05 \pm 0.02 \pm 0.01$	$0.21 \pm 0.10 \pm 0.04$
$D_s\bar{D}^{*0}K^-$	$0.30 \pm 0.18 \pm 0.06$	$0.09 \pm 0.05 \pm 0.02$	$0.31 \pm 0.21 \pm 0.06$	$D_s\bar{D}^{*0}K^{*-}$	$0.28 \pm 0.13 \pm 0.06$	$0.10 \pm 0.05 \pm 0.02$	$0.32 \pm 0.16 \pm 0.07$
$D_sD^{*-}\bar{K}^0$	$0.29 \pm 0.18 \pm 0.06$	$0.09 \pm 0.04 \pm 0.02$	$0.30 \pm 0.20 \pm 0.06$	$D_sD^{*-}\bar{K}^{*0}$	$0.27 \pm 0.13 \pm 0.06$	$0.09 \pm 0.04 \pm 0.02$	$0.31 \pm 0.15 \pm 0.07$
$D_s^*\bar{D}^{*0}K^-$	$0.89 \pm 0.59 \pm 0.18$	$0.17 \pm 0.09 \pm 0.03$	$0.65 \pm 0.39 \pm 0.14$	$D_s^*\bar{D}^{*0}K^{*-}$	$0.23 \pm 0.11 \pm 0.05$	$0.05 \pm 0.03 \pm 0.01$	$0.21 \pm 0.10 \pm 0.04$
$D_s^*D^{*-}\bar{K}^0$	$0.86 \pm 0.57 \pm 0.18$	$0.16 \pm 0.09 \pm 0.03$	$0.64 \pm 0.38 \pm 0.13$	$D_s^*D^{*-}\bar{K}^{*0}$	$0.21 \pm 0.10 \pm 0.04$	$0.05 \pm 0.03 \pm 0.01$	$0.20 \pm 0.09 \pm 0.04$
Total			$4.5 \pm 3.0 \pm 0.9$[a]	Total			$3.4 \pm 1.6 \pm 0.7$[a]

[a]The contribution from *CP*-conjugate modes is included.

modes with $\bar{K}$. If there is a measurement of modes in these two categories, it is possible to extract $\tilde{g}_{D_{sJ}D^{(*)}K^*}$ by fitting to branching fractions. The $\tilde{g}_{D_{sJ}D^{(*)}K^*}$ in return could help the identification of $D_{sJ}(2700)$. The current-produced modes with $\bar{K}^*$ have branching fractions on the order of 10^{-3}, similar to modes with $\bar{K}$.

The rise of branching fractions in current-produced modes leads to the increase of $\Delta\Gamma_s$. Following the trend of branching fractions, $\Delta\Gamma_f$ in Categories 2 and 4 have significant increases compared with the other two. In this scenario, the total $\Delta\Gamma_s/\Gamma_s$ is

$$\begin{aligned}\Delta\Gamma_s/\Gamma_s(D_s^{(*,**)}\bar{D}_s^{(*,**)}) &= (10.4 \pm 2.5 \pm 2.2)\%,\\ \Delta\Gamma_s/\Gamma_s(D_s^{(*)}\bar{D}^{(*)}\bar{K} + \bar{D}_s^{(*)}D^{(*)}K) &= (4.5 \pm 4.4 \pm 0.9)\%,\\ \Delta\Gamma_s/\Gamma_s(D_s^{(*)}\bar{D}^{(*)}\bar{K}^* + \bar{D}_s^{(*)}D^{(*)}K^*) &= (3.4 \pm 1.6 \pm 0.7)\%,\\ \Delta\Gamma_s/\Gamma_s &= (18.2 \pm 8.5 \pm 3.8)\%.\end{aligned} \tag{42}$$

The total $\Delta\Gamma_s$ induced by modes with $\bar{K}^*$ almost doubles. The effect from three-body modes is strengthen by considering the off-shell decay of $\bar{D}_{sJ}(2700)$ to $\bar{D}^{(*)}\bar{K}^*$. For total $\Delta\Gamma_s$, the central value returns to the one in Scenario I. Total $\Delta\Gamma_s$ does not alter significantly as the contribution for modes with $\bar{K}^*$ is not dominant. The result still agrees with the short-distance calculation.

The interference in modes with $\bar{K}^*$ is strong. Similar to the discussion in Scenario I, if we leave only $\bar{D}_{sJ}(2700)$ and turn off $\bar{D}_s^{(*)}$ poles, the resulting $\Delta\Gamma_f/\Gamma_s$ of these modes is only 0.3%. It is much smaller than the 1.5% increase found in Scenario III (compared to Scenario II). Recalling the result in Scenario I, one finds that modes with $\bar{K}^*$ allow more constructive interference than modes with $\bar{K}$. For modes with $\bar{K}$, the interference is restricted by the on-shell $\bar{D}_{sJ}(2700)$ resonance, which is localized in phase space. On the contrary, the $\bar{D}_{sJ}(2700)$ resonance becomes off-shell and hence smooth in phase space for modes with $\bar{K}^*$. It is more coherent to the $\bar{D}_s^{(*)}$ pole contributions and interferes with them better. As in the $\bar{K}$ case, the interference, mediated by the $\bar{D}^{(*)}\bar{K}^*$ pair, is comparable to the contribution of $\bar{D}_{sJ}(2700)$ itself.

We show that the branching fractions of these modes are on the order of 10^{-3} to 10^{-4}. Recall that there is no corresponding measurement in current-produced modes with $\bar{K}^*$ and in all transition modes. For current-produced modes with $\bar{K}^*$, they can be studied in the $\bar{B}_{u,d}$ system in analogy to modes with $\bar{K}$. These branching fractions should be measurable with current data collected by the B factories. On the other hand, $\bar{B}_{u,d}$ systems have different behaviors in transition modes. $B_{u,d}$ transit to $\bar{D}^{(*)}\pi$ pairs instead of to $\bar{D}^{(*)}\bar{K}^{(*)}$. The $\bar{D}^{(*)}\pi$ pairs can be produced either from nearly on-shell $\bar{D}^*$ or from other on-shell intermediate resonances. One expects the transition modes in $B_{u,d}$ are more enhanced than in B_s. In fact, semileptonic modes with $B_{u,d} \to \bar{D}^{(*)}\pi_{u,d}$ transition have been measured [34]. The branching fractions are around 0.5%, much larger than the transition modes in this work. For the purpose of estimating the width difference, $\Delta\Gamma_s$ can be bounded by Eq. (15d) when current-produced and transition modes are measured. Independent of $\Delta\Gamma_s$, experimental studies of these modes will be interesting enough in their own right.

So far, we fit the decay constant of $D_{sJ}(2700)$ by its contribution to $\bar{B}_u \to D_u\bar{D}^0K^-$ as measured by Belle. If future experiments favor the result of *BABAR* and lower the contribution of $D_{sJ}(2700)$, then the decay constant will be smaller. In such case, the branching fractions of modes in Categories 1 and 2 in the pole model become smaller and may be consistent with experiments without resorting to an

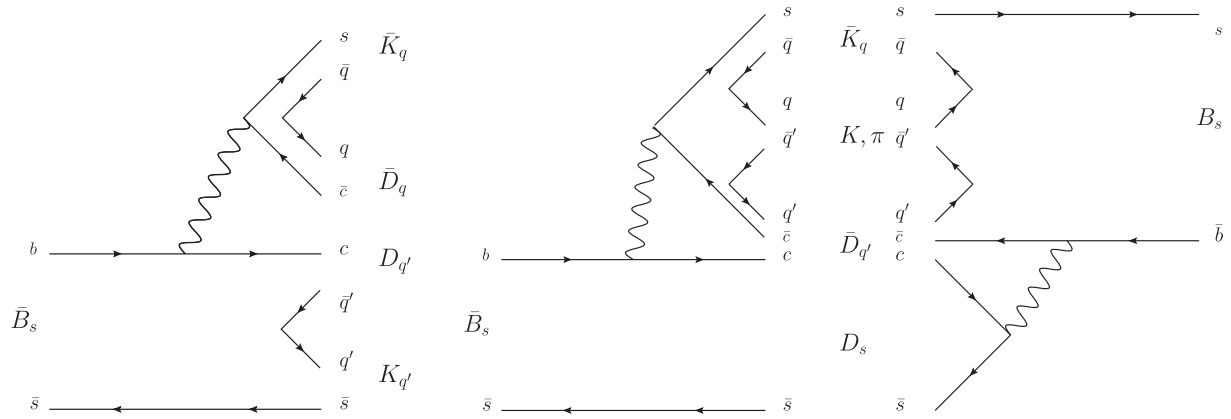

(a) 4-body diagram type I (b) 4-body diagram type II

FIG. 4. (a) The first type of four-body diagram. Both the current-produced and the transition parts have a $q\bar{q}$ pair. (b) The second type of four-body diagrams. All $q\bar{q}$ pairs lie in current (or in transition for B_s) decays to this mode.

NR contribution. Nevertheless, the branching fractions of modes in Categories 3 and 4 will be deficient. Similar to Scenario 2, one can then add NR contributions in the timelike form factors of $\bar{D}^*\bar{K}$ to fit the observed branching fractions. Although there are more NR parameters in $\bar{D}^*\bar{K}$ form factors, one can extract information in the Dalitz plots, especially the interference between the continuum and the $D_{sJ}(2700)$ resonance. These can be studied after future measurements are made.

In principle, modes with $s\bar{s}$, such as $\eta^{(\prime)}$, ω, and φ, can also contribute to $\Delta\Gamma_s$. These modes are difficult to calculate because they mix current-produced, transition, and color-suppressed diagrams together. Nonetheless, we find that the contributions of these modes are small. The phase space is suppressed and the number of modes is fewer. We estimate the contribution to $\Delta\Gamma_s$ by $D_s^{(*)}\bar{D}_s^{(*)}\eta^{(\prime)}$ modes with color-allowed diagrams only. The effect is less than 0.7%, which is negligible.

We have shown that the effect of three-body modes could be sizable. It will be interesting to see if other high-order modes could have a similar effect on $\Delta\Gamma_s$. Note that the phase space is gradually saturated from $D_s\bar{D}\,\bar{K}$ mode to $D_s^*\bar{D}^*\bar{K}^*$ mode, and the effect of high-order modes may be limited. Figure 4 shows the diagrams of possible four-body modes. The first type of diagram (left diagram in Fig. 4) can produce $D^{(*)}\bar{D}^{(*)}K^{(*)}\bar{K}^{(*)}$, but the two K mesons cannot be in excited states simultaneously because of insufficient phase space. The amplitude of this diagram can be calculated with the same form factors as in three-body modes. We roughly estimate the branching fraction of this type of diagram, which is 2 orders of magnitude smaller than 3-body modes. Given that the number of $D^{(*)}\bar{D}^{(*)}K^{(*)}\bar{K}^{(*)}$ modes is 48, only 0.5 times more than three-body diagrams, the contributions of these diagrams are still negligible. The second type may involve pions and could have a larger phase space. We calculate the dimensionless fraction of phase space area

$$\frac{1}{m_B^2}\frac{\mathcal{A}^\Phi(\text{four-body})}{\mathcal{A}^\Phi(\text{three-body})} < 10^{-4}, \tag{43}$$

where $\mathcal{A}^\Phi$ is the phase space area. This ratio strongly suggests that the effect of four-body modes is negligible. Even if the branching fractions of current amplitudes are large, the branching fraction of transition diagrams may not be as large as in current amplitudes. It should be safe to estimate $\Delta\Gamma_s$ up to three-body modes.

V. CONCLUSION

In conclusion, we have estimated the long-distance contribution to $\Delta\Gamma_s$ of the B_s-$\bar{B}_s$ system. First, we revisit the contributions by two-body $D_s^{(*)}\bar{D}_s^{(*)}$ modes. The $\Delta\Gamma_s/\Gamma_s$ by these modes is $(10.2 \pm 2.2 \pm 2.1)\%$, which is a decrease from the previous result in Ref. [21]. More precise measurements in the B_s system can help extract more accurate parameters and improve the theoretical prediction. After including $D_{s0}^*(2317)$, $D_{s1}(2460)$, and $D_{s1}(2536)$ resonances, the $\Delta\Gamma_s/\Gamma_s$ changes only slightly to $(10.4 \pm 2.5 \pm 2.2)\%$.

For the three-body $D_s^{(*)}\bar{D}^{(*)}\bar{K}^{(*)}$ modes, factorization formalism with form factors modeled by $\bar{D}_s^{(*)}$ and $\bar{D}_{sJ}(2700)$ poles and nonresonant (NR) contributions, if necessary, are used. The branching fractions predicted by pole models are consistent with experiment in two of the four categories, while agreement in the remaining modes with data can be achieved by including NR contribution. Three-body modes can bypass some difficulties in two-body modes. In particular, sizable constructive interference between $\bar{D}_{sJ}$ and $\bar{D}_s^{(*)}$ poles, which is impossible for two-body modes, is found.

Our results for $\Delta\Gamma_s$ in three scenarios are summarized in Eqs. (39), (40), and (42). Although the three scenarios have different theoretical assumptions, it is of interest to note that the resulting $\Delta\Gamma_s$ values are similar. Thus, we give the following concluding remarks. First, the total $\Delta\Gamma_s$ agrees with the short-distance calculation. In other words, long-distance contributions from $b \to c\bar{c}s$ decays do not enhance $\Delta\Gamma_s$ (or the real part of $\Gamma_{12,s}$) significantly. This demonstrates that the short-distance result and the assumption of OPE are reliable. If the anomalous dimuon asymmetry with sizable $\Delta\Gamma_s$ is confirmed in the future, the enhancement in $\Delta\Gamma_s$ must have origins from new physics.

Second, we find that the effect of three-body modes ($\sim$8%) is comparable to two-body modes ($\sim$10%). The assumption that two-body decays saturate $\Delta\Gamma_s$ receives a considerable correction. This correction comes from both $D_{sJ}(2700)$ and off-shell $D_s^{(*)}$ poles.

We end our conclusion by pointing out some experimental issues where progress can be made in the near future. Two-body modes in B_s decays need to be measured with better precision (see Sec. III A). For three-body modes, up to now, there has been no measurement of transition modes, nor of odes with K^* in the $B_{u,d}$ system. Even the available measurements in current-produced modes with K contain inconsistencies. In particular, the 2.2σ difference between Belle and *BABAR* in the $B^- \to D^0\bar{D}^0K^-$ mode has to be resolved. From the tables in Secs. III and IV, we see that many modes remain to be found or confirmed experimentally. For example, $\bar{B}_s \to D_s^*\bar{D}^{(*)}\bar{K}^{(*)}$ rates are predicted at the percent level and may be observed soon. Note that the modes with $\bar{D}^{(*)}\bar{K}^*$ will be useful for extracting the D_{sJ} strong coupling. Although the measurements of two- and three-body decay rates are useful for refining the theoretical prediction and to set a bound on $\Delta\Gamma_s$, these modes are of interest in their own right. We hope that (Super-) B factories and LHCb can complete the measurements of these missing modes.

ACKNOWLEDGMENTS

C.-K. C. thanks the National Science Council of Taiwan for support under Grants No. NSC-97-2112-M-033-002-MY3 and No. NSC-100-2112-M-033-001-MY3. W.-S. H. and C.-H. S. are grateful to the National Science Council of Taiwan for support through the Academic Summit Grant, No. NSC 99-2745-M-002-002-ASP.

Note added.—After the completion of this paper, we noticed the work of Ref. [42], which points out that penguin contributions to $B_s \to J/\psi\phi$ could somewhat reduce the need for enhanced $\Delta\Gamma_s$. It also reiterates the point made in the second reference of Ref. [3] that there is no indication of large or ill-behaved corrections to the short-distance expansion (or the heavy-quark expansion).

APPENDIX A: SOME CONVERSION AND TRANSFORMATION OF FORM FACTORS

Table IX provides the conversion of our notations to the usual notations of standard form factors.

If CP is conserved, the form factors of the current-produced particle pair and antiparticle pair can be related. For the standard form factors, the transformation reads

$$\begin{aligned}
f_{\bar{D}s,\bar{D}^*s,\bar{D}s1} &= +f_{Ds,D^*s,Ds1},\\
f_{\bar{D}s0,\bar{D}s1'} &= -f_{Ds0,Ds1'},\\
F_{0,1}^{Bs\bar{D}s}(q^2) &= -F_{0,1}^{\bar{B}sDs}(q^2),\\
F_{0,1}^{Bs\bar{D}s0}(q^2) &= +F_{0,1}^{\bar{B}sDs0}(q^2),\\
F_{0,1,2}^{Bs(\bar{D}^*s,\bar{D}s1)}(q^2) &= -F_{0,1,2}^{\bar{B}s(D^*s,Ds1)}(q^2),\\
F_{0,1,2}^{Bs\bar{D}s1'}(q^2) &= +F_{0,1,2}^{\bar{B}sDs1'}(q^2),\\
F_{3}^{Bs(\bar{D}^*s,\bar{D}s1)}(q^2) &= +F_{3}^{\bar{B}s(D^*s,Ds1)}(q^2),\\
F_{3}^{Bs\bar{D}s1'}(q^2) &= -F_{3}^{\bar{B}sDs1'}(q^2),
\end{aligned} \tag{A1}$$

where D_{s1} and $D_{s1'}$ are the CP-even and CP-odd states of the linear combination of $D_{s1}(2460)$ and $D_{s1}(2536)$. The relations for form factors in Eq. (21) to Eq. (23) are

$$\begin{aligned}
F_{0,1}^{PP}(q^2) &= -F_{0,1}^{\overline{PP}}(q^2),\\
V^{VP,VV}(q^2) &= +V^{\overline{VP},\overline{VV}}(q^2),\\
A^{VP,VV}(q^2) &= -A^{\overline{VP},\overline{VV}}(q^2).
\end{aligned} \tag{A2}$$

The transformations for transition form factors from Eq. (24) to Eq. (26) are

$$\begin{aligned}
V^{\bar{B}_sPP,\bar{B}_sVP,\bar{B}_sVV} &= -V^{B_s\overline{PP},B_s\overline{PP},B_s\overline{PP}},\\
A^{\bar{B}_sPP,\bar{B}_sVP,\bar{B}_sVV} &= +A^{B_s\overline{PP},B_s\overline{VP},B_s\overline{VV}}.
\end{aligned} \tag{A3}$$

Compared with Eq. (A2), there is one additional minus sign coming from the pseudoscalar B_s meson.

TABLE IX. The conversion of the form-factors notation in this work to the usual notation in the literature.

	D_s	D_{s0}	D_s^*	$D_{s1}(2460, 2536)$
$f_{\mathcal{D}(*)s}$	f_{Ds}	f_{Ds0}	f_{D^*s}	$-f_{Ds1}$
$F_1^{\bar{B}_s\mathcal{D}s}$	$F_1^{\bar{B}_sDs}$	$-F_1^{\bar{B}_sDs0}$		
$F_0^{\bar{B}_s\mathcal{D}s}$	$F_0^{\bar{B}_sDs}$	$-F_0^{\bar{B}_sDs0}$		
$F_3^{\bar{B}_s\mathcal{D}^*s}$			$V^{\bar{B}_sD^*s}$	$-\frac{m_{Bs}+m_{Ds1}}{m_{Bs}-m_{Ds1}}A^{\bar{B}_sD^*s0}$
$F_1^{\bar{B}_s\mathcal{D}^*s}$			$A_1^{\bar{B}_sD^*s}$	$\frac{m_{Bs}-m_{Ds1}}{m_{Bs}+m_{Ds1}}V_1^{\bar{B}_sD^*s0}$
$F_2^{\bar{B}_s\mathcal{D}^*s}$			$A_2^{\bar{B}_sD^*s}$	$\frac{m_{Bs}+m_{Ds1}}{m_{Bs}-m_{Ds1}}V_2^{\bar{B}_sD^*s0}$
$F_0^{\bar{B}_s\mathcal{D}^*s}$			$A_0^{\bar{B}_sD^*s}$	$V_0^{\bar{B}_sD^*s0}$

APPENDIX B: POLE CONTRIBUTION TO FORM FACTORS

For simplicity, we list only the contributions from D_s and D_s^* poles. The contributions of $D_{sJ}(2700)$ have the same forms as D_s^*, but with different mass, width, and strong coupling constants.

In the timelike DK transition form factors, D_s^* is the only possible pole. But there is an ambiguity in the matrix element $\langle DK|i\mathcal{L}_{\rm eff}|D_{\rm int}^*\rangle$ when D^* goes to off shell. The matrix element is given by

$$\begin{aligned}
&\langle D(p_D)K(p_K)|i\mathcal{L}_{\rm eff}|D_{\rm int}^*(p_{D^*},\varepsilon_{D^*})\rangle\\
&\quad = \varepsilon_{\rm int}\cdot\left(\frac{1}{2}(p_K-p_D)+\alpha q\right),
\end{aligned} \tag{B1}$$

where α is undetermined since the associated term is zero when D_s^* is on shell. According to this matrix element, the pole contribution to the timelike form factor becomes

$$\begin{aligned}
F_1^{DK}(q^2) &= \frac{g_{D^*DP}f_{D_{\rm int}^*}m_{\rm int*}}{q^2-m_{\rm int*}^2+im_{\rm int*}\Gamma_{\rm int*}}\frac{1}{2},\\
F_0^{DK}(q^2) &= \frac{g_{D^*DP}f_{D_{\rm int}^*}m_{\rm int*}}{q^2-m_{\rm int*}^2+im_{\rm int*}\Gamma_{\rm int*}}\\
&\quad\times\left(\frac{q^2-m_{\rm int*}^2}{m_{\rm int*}^2}\left(\frac{q^2}{m_D^2-m_K^2}\alpha-\frac{1}{2}\right)\right),
\end{aligned} \tag{B2}$$

where $m_{\rm int*}$ and $\Gamma_{\rm int*}$ are the mass and width of the D_s^* pole, respectively. If α is nonzero, $A_0^{DK}(q^2)$ will increase as q^2 increases. Such energy dependence is unnatural for form factors. We hence set α as zero. Once α is fixed, we have the following pole contribution to transition form factors,

$$
\begin{aligned}
\frac{V^{\bar{B}_s DK}}{m_{B_s}^3} &= \left(\frac{g_{D^*DP}}{q^2 - m_{\mathrm{int}*}^2 + i m_{\mathrm{int}*}\Gamma_{\mathrm{int}*}}\right)\frac{1}{2}\frac{2V^{\bar{B}_s D^*}}{m_{B_s} + m_{\mathrm{int}*}},\\
\frac{A_1^{\bar{B}_s DK}}{m_{B_s}} &= \left(\frac{g_{D^*DP}}{q^2 - m_{\mathrm{int}*}^2 + i m_{\mathrm{int}*}\Gamma_{\mathrm{int}*}}\right)\frac{q'^2}{2(q'^2 + q^2 - m_{B_s}^2)}\left(q'(p_D - p_K) - \frac{m_D^2 - m_K^2}{m_{\mathrm{int}*}^2}qq'\right)\\
&\quad\times\left(\frac{m_{B_s} + m_{\mathrm{int}*}}{q'^2}A_1^{\bar{B}_s D^*} + \left(1 - \frac{m_{B_s}^2 - m_{\mathrm{int}*}^2}{q'^2}\right)\frac{A_2^{\bar{B}_s D^*}}{m_{B_s} + m_{\mathrm{int}*}} - \frac{2m_{\mathrm{int}*}}{q'^2}A_0^{\bar{B}_s D^*}\right),\\
\frac{A_2^{\bar{B}_s DK}}{m_{B_s}} &= \left(\frac{g_{D^*DP}}{q^2 - m_{\mathrm{int}*}^2 + i m_{\mathrm{int}*}\Gamma_{\mathrm{int}*}}\right)\frac{-1}{2}(m_{B_s} + m_{\mathrm{int}*})A_1^{\bar{B}_s D^*},\\
\frac{A_0^{\bar{B}_s DK}}{m_{B_s}} &= \left(\frac{g_{D^*DP}}{q^2 - m_{\mathrm{int}*}^2 + i m_{\mathrm{int}*}\Gamma_{\mathrm{int}*}}\right)\left\{\frac{q^2}{m_D^2 - m_K^2}\left[\frac{m_D^2 - m_K^2}{2m_{\mathrm{int}*}^2}(m_{B_s} + m_{\mathrm{int}*})A_1^{\bar{B}_s D^*}\right.\right.\\
&\quad\left.\left. + \left(q'(p_D - p_K) - \frac{m_D^2 - m_K^2}{m_{\mathrm{int}*}^2}qq'\right)\frac{A_2^{\bar{B}_s D^*}}{m_{B_s} + m_{\mathrm{int}*}} - 2\frac{A_1^{\bar{B}_s DK}}{m_{B_s}}\right] + \frac{A_2^{\bar{B}_s DK}}{m_{B_s}}\right\},
\end{aligned}
\tag{B3}
$$

where $q = p_D + p_K$ is the total momentum of transited mesons, and $q' = p_{\bar{B}_s} - q$ is the momentum of weak current.

Other modes receive contribution from both D_s and D_s^* poles. The timelike form factors of D^*K are

$$
\begin{aligned}
\frac{2V^{D^*K}(q^2)}{m_{D^*} + m_K} &= \left(\frac{-g_{D^*D^*P}f_{D_{\mathrm{int}}^*}m_{\mathrm{int}*}}{q^2 - m_{\mathrm{int}*}^2 + i m_{\mathrm{int}*}\Gamma_{\mathrm{int}*}}\right),\\
A_1^{D^*K}(q^2) &= 0,\\
A_2^{D^*K}(q^2) &= 0,\\
2m_{D^*}A_0^{D^*K}(q^2) &= \left(\frac{g_{D^*DP}f_{D_{\mathrm{int}}}}{q^2 - m_{\mathrm{int}}^2 + i m_{\mathrm{int}}\Gamma_{\mathrm{int}}}\right)q^2,
\end{aligned}
\tag{B4}
$$

where $m_{\mathrm{int}(*)}$ and $\Gamma_{\mathrm{int}(*)}$ are the mass and width of the $D_s^{(*)}$ poles, respectively. The $\bar{B}_s$ to D^*K transition form factors induced by $D_s^{(*)}$ poles are given by

$$
\begin{aligned}
\frac{V_2^{\bar{B}_s D^*K}}{m_{B_s}^2} &= \left(\frac{g_{D^*D^*P}}{q^2 - m_{\mathrm{int}*}^2 + i m_{\mathrm{int}*}\Gamma_{\mathrm{int}*}}\right)(m_{B_s} + m_{\mathrm{int}*})A_1^{\bar{B}_s D^*},\\
\frac{V_1^{\bar{B}_s D^*K}}{m_{B_s}^4} &= \left(\frac{g_{D^*D^*P}}{q^2 - m_{\mathrm{int}*}^2 + i m_{\mathrm{int}*}\Gamma_{\mathrm{int}*}}\right)\frac{A_2^{\bar{B}_s D^*}}{(m_{B_s} + m_{\mathrm{int}*})},\\
\frac{V_0^{\bar{B}_s D^*K}}{m_{B_s}^2} &= \left(\frac{-g_{D^*D^*P}}{q^2 - m_{\mathrm{int}*}^2 + i m_{\mathrm{int}*}\Gamma_{\mathrm{int}*}}\right)(2m_{\mathrm{int}*})A_0^{\bar{B}_s D^*} - (q^2 - m_{\mathrm{int}*}^2)\frac{V_1^{\bar{B}_s D^*K}}{m_{B_s}^4},\\
\frac{A_3^{\bar{B}_s D^*K}}{m_{B_s}^4} &= \left(\frac{g_{D^*D^*P}}{q^2 - m_{\mathrm{int}*}^2 + i m_{\mathrm{int}*}\Gamma_{\mathrm{int}*}}\right)\frac{2V^{\bar{B}_s D^*}}{(m_{B_s} + m_{\mathrm{int}*})},\\
\frac{A_1^{\bar{B}_s D^*K}}{m_{B_s}^2} &= \left(\frac{-g_{D^*DP}}{q^2 - m_{\mathrm{int}}^2 + i m_{\mathrm{int}}\Gamma_{\mathrm{int}}}\right)A_1^{\bar{B}_s D},\\
\frac{A_0^{\bar{B}_s D^*K}}{m_{B_s}^2} &= \left(\frac{m_{B_s}^2 - m_{\mathrm{int}}^2}{m_{B_s}^2 - q^2}\right)\left(\frac{-g_{D^*DP}}{q^2 - m_{\mathrm{int}}^2 + i m_{\mathrm{int}}\Gamma_{\mathrm{int}}}\right)A_0^{\bar{B}_s D} - \left(\frac{q^2 - m_{\mathrm{int}}^2}{m_{B_s}^2 - q^2}\right)\frac{A_1^{\bar{B}_s D^*K}}{m_{B_s}^2}.
\end{aligned}
\tag{B5}
$$

The DK^* and D^*K form factors are parametrized in the same way. The pole parts of the DK^* timelike form factors are

$$\begin{aligned}
\frac{2V^{DK^*}(q^2)}{m_D + m_{K^*}} &= \left(\frac{4f_{D^*DV}f_{D^*_{\rm int}}m_{{\rm int}*}}{q^2 - m^2_{{\rm int}*} + im_{{\rm int}*}\Gamma_{{\rm int}*}}\right),\\
A_1^{DK^*}(q^2) &= 0,\\
A_2^{DK^*}(q^2) &= 0,\\
2m_{K^*}A_0^{DK^*}(q^2) &= -2q^2\left(\frac{g_{DDV}f_{D_{\rm int}}}{q^2 - m^2_{\rm int} + im_{\rm int}\Gamma_{\rm int}}\right).
\end{aligned} \tag{B6}$$

And the transition form factors derived from the pole model are written as

$$\begin{aligned}
\frac{V_2^{\bar{B}_sDK^*}}{m^2_{B_s}} &= \left(\frac{-4f_{D^*DV}}{q^2 - m^2_{{\rm int}*} + im_{{\rm int}*}\Gamma_{{\rm int}*}}\right)(m_{B_s} + m_{{\rm int}*})A_1^{\bar{B}_sD^*},\\
\frac{V_1^{\bar{B}_sDK^*}}{m^4_{B_s}} &= \left(\frac{-4f_{D^*DV}}{q^2 - m^2_{{\rm int}*} + im_{{\rm int}*}\Gamma_{{\rm int}*}}\right)\frac{A_2^{\bar{B}_sD^*}}{(m_{B_s} + m_{{\rm int}*})},\\
\frac{V_0^{\bar{B}_sDK^*}}{m^2_{B_s}} &= \left(\frac{4f_{D^*DV}}{q^2 - m^2_{{\rm int}*} + im_{{\rm int}*}\Gamma_{{\rm int}*}}\right)(2m_{{\rm int}*})A_0^{\bar{B}_sD^*} - (q^2 - m^2_{{\rm int}*})\frac{V_1^{\bar{B}_sDK^*}}{m^4_{B_s}},\\
\frac{A_3^{\bar{B}_sDK^*}}{m^4_{B_s}} &= \left(\frac{-4f_{D^*DV}}{q^2 - m^2_{{\rm int}*} + im_{{\rm int}*}\Gamma_{{\rm int}*}}\right)\frac{2V^{\bar{B}_sD^*}}{(m_{B_s} + m_{{\rm int}*})},\\
\frac{A_1^{\bar{B}_sDK^*}}{m^2_{B_s}} &= \left(\frac{2g_{DDV}}{q^2 - m^2_{\rm int} + im_{\rm int}\Gamma_{\rm int}}\right)A_1^{\bar{B}_sD},\\
\frac{A_0^{\bar{B}_sDK^*}}{m^2_{B_s}} &= \left(\frac{m^2_{B_s} - m^2_{\rm int}}{m^2_{B_s} - q^2}\right)\left(\frac{2g_{DDV}}{q^2 - m^2_{\rm int} + im_{\rm int}\Gamma_{\rm int}}\right)A_0^{\bar{B}_sD} - \left(\frac{q^2 - m^2_{\rm int}}{m^2_{B_s} - q^2}\right)\frac{A_1^{\bar{B}_sDK^*}}{m^2_{B_s}}.
\end{aligned} \tag{B7}$$

Finally, the form factors from $D_s^{(*)}$ poles are

$$\begin{aligned}
\frac{V_0^{D^*K^*}(q^2)}{(m_{D^*} + m_{K^*})^2} &= \left(\frac{-4f_{D^*DV}f_{\rm int}}{q^2 - m^2_{\rm int} + im_{\rm int}\Gamma_{\rm int}}\right),\\
\frac{V_1^{D^*K^*}(q^2)}{(m_{D^*} + m_{K^*})^2} &= 0,\\
\frac{V_2^{D^*K^*}(q^2)}{(m_{D^*} + m_{K^*})^2} &= 0,\\
A_{11}^{D^*K^*}(q^2) &= \left(\frac{2g_{D^*D^*V}m_{{\rm int}*}f_{{\rm int}*}}{q^2 - m^2_{{\rm int}*} + im_{{\rm int}*}\Gamma_{{\rm int}*}}\right),\\
A_{12}^{D^*K^*}(q^2) &= \left(\frac{-4f_{D^*D^*V}m_{{\rm int}*}f_{{\rm int}*}}{q^2 - m^2_{{\rm int}*} + im_{{\rm int}*}\Gamma_{{\rm int}*}}\right),\\
A_2^{D^*K^*}(q^2) &= \left(\frac{-2f_{D^*D^*V}m_{{\rm int}*}f_{{\rm int}*}}{q^2 - m^2_{{\rm int}*} + im_{{\rm int}*}\Gamma_{{\rm int}*}}\right),\\
A_{01}^{D^*K^*}(q^2) &= \left(\frac{-2g_{D^*D^*V}m_{{\rm int}*}f_{{\rm int}*}}{q^2 - m^2_{{\rm int}*} + im_{{\rm int}*}\Gamma_{{\rm int}*}}\right)\frac{q^2}{m^2_{{\rm int}*}} + \left(\frac{4f_{D^*D^*V}m_{{\rm int}*}f_{{\rm int}*}}{q^2 - m^2_{{\rm int}*} + im_{{\rm int}*}\Gamma_{{\rm int}*}}\right)\frac{q^2}{m^2_{\rm int}} + A_{11}^{D^*K^*}(q^2) + A_{12}^{D^*K^*}(q^2),\\
A_{02}^{D^*K^*}(q^2) &= \left(\frac{4f_{D^*D^*V}m_{{\rm int}*}f_{{\rm int}*}}{q^2 - m^2_{{\rm int}*} + im_{{\rm int}*}\Gamma_{{\rm int}*}}\right)\left(\frac{1}{2} - \frac{q^2 - m^2_{D^*} + m^2_{K^*}}{2m^2_{{\rm int}*}}\right)\frac{q^2}{(m_{D^*} + m_{K^*})^2} + \left(\frac{m^2_{D^*} - m^2_{K^*}}{q^2}\right)A_2^{D^*K^*}(q^2).
\end{aligned} \tag{B8}$$

And the transition form factors are given by the following three equations. The first part is the form factors from the vector current:

$$
\begin{aligned}
\frac{V_3^{\bar{B}_s D^* K^*}}{m_{B_s}^3} &= \left(\frac{4 f_{D^* D^* V}}{q^2 - m_{\mathrm{int}*}^2 + i m_{\mathrm{int}*}\Gamma_{\mathrm{int}*}}\right)\frac{2V^{\bar{B}_s D^*}}{m_{B_s} + m_{\mathrm{int}*}},\\
\frac{V_2^{\bar{B}_s D^* K^*}}{m_{B_s}^3} &= \left(\frac{2 g_{D^* D^* V}}{q^2 - m_{\mathrm{int}*}^2 + i m_{\mathrm{int}*}\Gamma_{\mathrm{int}*}}\right)\frac{2V^{\bar{B}_s D^*}}{m_{B_s} + m_{\mathrm{int}*}},\\
\frac{V_1^{\bar{B}_s D^* K^*}}{m_{B_s}^3} &= \left(\frac{4 f_{D^* D^* V}}{q^2 - m_{\mathrm{int}*}^2 + i m_{\mathrm{int}*}\Gamma_{\mathrm{int}*}}\right)\left(-\frac{2V^{\bar{B}_s D^*}}{m_{B_s} + m_{\mathrm{int}*}}\right),\\
\frac{V_{01}^{\bar{B}_s D^* K^*}}{m_{B_s}^3} &= \left(\frac{-4 f_{D^* D V}}{q^2 - m_{\mathrm{int}}^2 + i m_{\mathrm{int}}\Gamma_{\mathrm{int}}}\right)A_1^{\bar{B}_s D},\\
\frac{V_{00}^{\bar{B}_s D^* K^*}}{m_{B_s}^3} &= \left(\frac{-4 f_{D^* D V}}{q^2 - m_{\mathrm{int}}^2 + i m_{\mathrm{int}}\Gamma_{\mathrm{int}}}\right)A_0^{\bar{B}_s D}.
\end{aligned}
\tag{B9}
$$

The second part originates from axial currents:

$$
\begin{aligned}
\frac{A_{62}^{\bar{B}_s D^* K^*}}{m_{B_s}} &= \left(\frac{4 f_{D^* D^* V}}{q^2 - m_{\mathrm{int}*}^2 + i m_{\mathrm{int}*}\Gamma_{\mathrm{int}*}}\right)\frac{1}{2}(m_{B_s} + m_{\mathrm{int}*})A_1^{\bar{B}_s D^*},\\
\frac{A_{61}^{\bar{B}_s D^* K^*}}{m_{B_s}} &= \left(\frac{4 f_{D^* D^* V}}{q^2 - m_{\mathrm{int}*}^2 + i m_{\mathrm{int}*}\Gamma_{\mathrm{int}*}}\right)\left\{-\left(-q' p_{K^*} + \frac{q q' \cdot q p_{K^*}}{m_{\mathrm{int}*}^2}\right)\frac{A_2^{\bar{B}_s D^*}}{m_{B_s} + m_{\mathrm{int}*}} + \frac{q p_{K^*}}{2 m_{\mathrm{int}*}^2}(m_{B_s} + m_{\mathrm{int}*})A_1^{\bar{B}_s D^*}\right\}\\
&\quad - \frac{1}{2}\left(1 - \frac{m_{D^*}^2 - m_{K^*}^2}{q^2}\right)\frac{A_{62}^{\bar{B}_s D^* K^*}}{m_{B_s}},\\
m_{B_s} A_{60}^{\bar{B}_s D^* K^*} &= \left(\frac{4 f_{D^* D^* V}}{q^2 - m_{\mathrm{int}*}^2 + i m_{\mathrm{int}*}\Gamma_{\mathrm{int}*}}\right)\left(-q' p_{K^*} + \frac{q q' \cdot q p_{K^*}}{m_{\mathrm{int}*}^2}\right)\left\{-(m_{B_s} + m_{\mathrm{int}*})A_1^{\bar{B}_s D^*} + 2 m_{\mathrm{int}*} A_0^{\bar{B}_s D^*}\right.\\
&\quad \left. - (q'^2 - (m_{B_s}^2 - m_{\mathrm{int}*}^2))\frac{A_2^{\bar{B}_s D^*}}{m_{B_s} + m_{\mathrm{int}*}}\right\} - (q'^2 - (m_{B_s}^2 - q^2))\frac{A_{61}^{\bar{B}_s D^* K^*}}{m_{B_s}},
\end{aligned}
\tag{B10}
$$

$$
\begin{aligned}
\frac{A_3^{\bar{B}_s D^* K^*}}{m_{B_s}} &= \left(\frac{-2 g_{D^* D^* V} m_{\mathrm{int}*} f_{\mathrm{int}*}}{q^2 - m_{\mathrm{int}*}^2 + i m_{\mathrm{int}*}\Gamma_{\mathrm{int}*}}\right)(m_{B_s} + m_{\mathrm{int}*})A_1^{\bar{B}_s D^*},\\
\frac{A_4^{\bar{B}_s D^* K^*}}{m_{B_s}} &= \left(\frac{4 f_{D^* D^* V}}{q^2 - m_{\mathrm{int}*}^2 + i m_{\mathrm{int}*}\Gamma_{\mathrm{int}*}}\right)(m_{B_s} + m_{\mathrm{int}*})A_1^{\bar{B}_s D^*},\\
\frac{A_{21}^{\bar{B}_s D^* K^*}}{m_{B_s}^3} &= \left(\frac{-2 g_{D^* D^* V} m_{\mathrm{int}*} f_{\mathrm{int}*}}{q^2 - m_{\mathrm{int}*}^2 + i m_{\mathrm{int}*}\Gamma_{\mathrm{int}*}}\right)\frac{-A_2^{\bar{B}_s D^*}}{m_{B_s} + m_{\mathrm{int}*}},\\
\frac{A_{20}^{\bar{B}_s D^* K^*}}{m_{B_s}} &= \left(\frac{-2 g_{D^* D^* V} m_{\mathrm{int}*} f_{\mathrm{int}*}}{q^2 - m_{\mathrm{int}*}^2 + i m_{\mathrm{int}*}\Gamma_{\mathrm{int}*}}\right)\left\{-(m_{B_s} + m_{\mathrm{int}*})A_1^{\bar{B}_s D^*}\right.\\
&\quad \left. - (q'^2 - (m_{B_s}^2 - m_{\mathrm{int}*}^2))\frac{A_2^{\bar{B}_s D^*}}{m_{B_s} + m_{\mathrm{int}*}} + 2 m_{\mathrm{int}*} A_0^{\bar{B}_s D^*}\right\} - (q'^2 - (m_{B_s}^2 - q^2))\frac{A_{21}^{\bar{B}_s D^* K^*}}{m_{B_s}^3},,
\end{aligned}
\tag{B11}
$$

and

$$
\begin{aligned}
\frac{A_{11}^{\bar{B}_s D^* K^*}}{m_{B_s}^3} &= \left(\frac{4 f_{D^* D^* V}}{q^2 - m_{\mathrm{int}*}^2 + i m_{\mathrm{int}*}\Gamma_{\mathrm{int}*}}\right)\frac{-A_2^{\bar{B}_s D^*}}{m_{B_s} + m_{\mathrm{int}*}},\\
\frac{A_{10}^{\bar{B}_s D^* K^*}}{m_{B_s}} &= \left(\frac{4 f_{D^* D^* V}}{q^2 - m_{\mathrm{int}*}^2 + i m_{\mathrm{int}*}\Gamma_{\mathrm{int}*}}\right)\left\{-(m_{B_s} + m_{\mathrm{int}*})A_1^{\bar{B}_s D^*} - (q'^2 - (m_{B_s}^2 - m_{\mathrm{int}*}^2))\frac{A_2^{\bar{B}_s D^*}}{m_{B_s} + m_{\mathrm{int}*}} + 2 m_{\mathrm{int}*} A_0^{\bar{B}_s D^*}\right\}\\
&\quad - (q'^2 - (m_{B_s}^2 - q^2))\frac{A_{11}^{\bar{B}_s D^* K^*}}{m_{B_s}^3},
\end{aligned}
\tag{B12}
$$

TABLE X. The transition form factors for $\bar{B}_s \to D_s^{(*)}$ used in this work.

	$F(0)$	a	b
$F_0^{\bar{B}_s D_s}$	0.67 ± 0.03	0.58	0.06
$F_1^{\bar{B}_s D_s}$	0.67 ± 0.03	1.24	0.46
$V^{\bar{B}_s D_s^*}$	0.77 ± 0.04	1.42	0.68
$A_0^{\bar{B}_s D_s^*}$	0.65 ± 0.03	1.37	0.63
$A_1^{\bar{B}_s D_s^*}$	0.62 ± 0.03	0.77	0.11
$A_2^{\bar{B}_s D_s^*}$	0.59 ± 0.03	1.27	0.56

$$\frac{A_{01}^{\bar{B}_s D^* K^*}}{m_{B_s}^3} = \left\{\frac{-2 g_{D^* D^* V} m_{\mathrm{int}*} f_{\mathrm{int}*}}{q^2 - m_{\mathrm{int}*}^2 + i m_{\mathrm{int}*}\Gamma_{\mathrm{int}*}} + \frac{4 f_{D^* D^* V}}{q^2 - m_{\mathrm{int}*}^2 + i m_{\mathrm{int}*}\Gamma_{\mathrm{int}*}}\right\}\left\{\frac{-1}{2 m_{\mathrm{int}*}^2}(m_{B_s} + m_{\mathrm{int}*}) A_1^{\bar{B}_s D^*} + \frac{q q'}{m_{\mathrm{int}*}^2}\frac{A_2^{\bar{B}_s D^*}}{m_{B_s} + m_{\mathrm{int}*}}\right\}$$
$$+ \frac{1}{2q^2}\left(\frac{A_3^{\bar{B}_s D^* K^*}}{m_{B_s}} + \frac{A_4^{\bar{B}_s D^* K^*}}{m_{B_s}}\right),$$
$$\frac{A_{00}^{\bar{B}_s D^* K^*}}{m_{B_s}} = \left\{\frac{-2 g_{D^* D^* V} m_{\mathrm{int}*} f_{\mathrm{int}*}}{q^2 - m_{\mathrm{int}*}^2 + i m_{\mathrm{int}*}\Gamma_{\mathrm{int}*}} + \frac{4 f_{D^* D^* V}}{q^2 - m_{\mathrm{int}*}^2 + i m_{\mathrm{int}*}\Gamma_{\mathrm{int}*}}\right\}\frac{q q'}{m_{\mathrm{int}*}^2}$$
$$\times \left\{(m_{B_s} + m_{\mathrm{int}*}) A_1^{\bar{B}_s D^*} + (q'^2 - (m_{B_s}^2 - m_{\mathrm{int}*}^2))\frac{A_2^{\bar{B}_s D^*}}{m_{B_s} + m_{\mathrm{int}*}} - 2 m_{\mathrm{int}*} A_0^{\bar{B}_s D^*}\right\} - (q'^2 - (m_{B_s}^2 - q^2))\frac{A_{01}^{\bar{B}_s D^* K^*}}{m_{B_s}^3}. \quad \text{(B13)}$$

APPENDIX C: BASIC DECAY CONSTANTS AND FORM FACTORS

The values of basic parameters are summarized in this section. We take Wilson coefficients $c_1 = 1.081$ and $c_2 = -0.190$ with naïve factorization. This corresponds to

$$a_1 = 1.02 \pm 0.10, \quad \text{(C1)}$$

where we estimate a 10% uncertainty. The decay constants of $D_{u,d}$ and form factors of $\bar{B}_{u,d} \to D_{u,d}$ are given in Ref. [29].

For calculating $\bar{B}_s \to D_s^{(*)}$ transition form factors, we use the same method as in Ref. [29]. The $D_s^{(*)}$ decay constants are taken to be

$$f_{D_s} = 260 \pm 13 \text{ MeV}, \qquad f_{D_s^*} = 260 \pm 13 \text{ MeV}. \quad \text{(C2)}$$

The decay constant of D_s is consistent with the measured values in Ref. [34]. The decay constant of D_s^* should be the same as D_s in the heavy-quark limit. Using these two decay constants as constraints, we calculate the transition form factor, which is parametrized as

$$F^{\bar{B}_s D_s^{(*)}}(q^2) = \frac{F(0)}{1 - a q^2 + b q^4}. \quad \text{(C3)}$$

The three parameters $F(0)$, a, and b of different form factors are given in Table X.

[1] V. M. Abazov *et al.* (D0 Collaboration), Phys. Rev. D **82**, 032001 (2010); Phys. Rev. Lett. **105**, 081801 (2010).
[2] V. M. Abazov *et al.* (D0 Collaboration), Phys. Rev. D, **84**, 052007 (2011).
[3] A. Lenz and U. Nierste, J. High Energy Phys. 06 (2007) 072; updates in arXiv:1102.4274.
[4] D. Asner *et al.* (Heavy Flavor Averaging Group Collaboration), arXiv:1010.1589; online update at [http://www.slac.stanford.edu/xorg/hfag].
[5] Z. Ligeti, M. Papucci, G. Perez, and J. Zupan, Phys. Rev. Lett. **105**, 131601 (2010).
[6] N. G. Deshpande, X. G. He, and G. Valencia, Phys. Rev. D **82**, 056013 (2010).
[7] C. W. Bauer and N. D. Dunn, Phys. Lett. B **696**, 362 (2011).
[8] C.-H. Chen, C.-Q. Geng, and W. Wang, J. High Energy Phys. 11 (2010) 089.
[9] A. J. Buras, M. V. Carlucci, S. Gori, and G. Isidori, J. High Energy Phys. 10 (2010) 009.
[10] A. Lenz *et al.*, Phys. Rev. D **83**, 036004 (2011).
[11] A. Dighe, A. Kundu, and S. Nandi, Phys. Rev. D **82**, 031502 (2010).

[12] B. A. Dobrescu, P. J. Fox, and A. Martin, Phys. Rev. Lett. **105**, 041801 (2010).

[13] J. K. Parry, Phys. Lett. B **694**, 363 (2011); P. Ko and J.-h. Park, Phys. Rev. D **82**, 117701 (2010); J. Kubo and A. Lenz, *ibid.* **82**, 075001 (2010).

[14] Y. Bai and A. E. Nelson, Phys. Rev. D **82**, 114027 (2010).

[15] B. Dutta, Y. Mimura, and Y. Santoso, Phys. Rev. D **82**, 055017 (2010).

[16] S. Oh and J. Tandean, Phys. Lett. B **697**, 41 (2011).

[17] C.-H. Chen and G. Faisel, Phys. Lett. B **696**, 487 (2011).

[18] W.-S. Hou and N. Mahajan, Phys. Rev. D **75**, 077501 (2007); see also G. W.-S. Hou, in *Proceedings of TOP2010, Bruges, Belgium*, arXiv:1007.2288.

[19] D0 Collaboration, D0 Report No. 6098-CONF; the combined result is given by D0 Report No. 6093.

[20] G. Ciurgiu, Proc. Sci., ICHEP2010 (2010) 236; CDF Collaboration, CDF Report No. 10206.

[21] R. Aleksan, A. Le Yaouanc, L. Oliver, O. Pene, and J. C. Raynal, Phys. Lett. B **316**, 567 (1993).

[22] I. Dunietz, R. Fleischer, and U. Nierste, Phys. Rev. D **63**, 114015 (2001).

[23] C.-K. Chua, W.-S. Hou, S.-Y. Shiau, and S.-Y. Tsai, Phys. Rev. D **67**, 034012 (2003); C.-K. Chua, W.-S. Hou, and S.-Y. Tsai, *ibid.* **70**, 034032 (2004).

[24] B. Aubert *et al.* (*BABAR* Collaboration), Phys. Rev. D **68**, 092001 (2003).

[25] B. Aubert *et al.* (*BABAR* Collaboration), Phys. Rev. D **74**, 091101 (2006); J. Dalseno *et al.* (Belle Collaboration), *ibid.* **76**, 072004 (2007).

[26] J. Brodzicka *et al.* (Belle Collaboration), Phys. Rev. Lett. **100**, 092001 (2008).

[27] B. Aubert *et al.* (*BABAR* Collaboration), Phys. Rev. D **77**, 011102 (2008).

[28] P. del Amo Sanchez *et al.* (*BABAR* Collaboration), Phys. Rev. D **83**, 032004 (2011).

[29] H.-Y. Cheng, C.-K. Chua, and C.-W. Hwang, Phys. Rev. D **69**, 074025 (2004).

[30] C.-L. Lee, M. Lu, and M. B. Wise, Phys. Rev. D **46**, 5040 (1992).

[31] T.-M. Yan *et al.*, Phys. Rev. D **46**, 1148 (1992); **55**, 5851 (E) (1997).

[32] R. Casalbuoni *et al.*, Phys. Rep. **281**, 145 (1997).

[33] H.-Y. Cheng, C.-K. Chua, and A. Soni, Phys. Rev. D **71**, 014030 (2005).

[34] K. Nakamura *et al.* (Particle Data Group), J. Phys. G **37**, 075021 (2010); and 2011 partial update for the 2012 edition [http://pdg.lbl.gov].

[35] B. Aubert *et al.* (*BABAR* Collaboration), Phys. Rev. D **80**, 092003 (2009).

[36] S. Godfrey and N. Isgur, Phys. Rev. D **32**, 189 (1985); D. Ebert, R. N. Faustov, and V. O. Galkin, Eur. Phys. J. C **66**, 197 (2010); T. Matsuki, T. Morii, and K. Sudoh, Eur. Phys. J. A **31**, 701 (2007); A. M. Badalian and B. L. G. Bakker, Phys. Rev. D **84**, 034006 (2011).

[37] P. Colangelo, F. De Fazio, S. Nicotri, and M. Rizzi, Phys. Rev. D **77**, 014012 (2008).

[38] G.-L. Wang, J.-M. Zhang, and Z.-H. Wang, Phys. Lett. B **681**, 326 (2009).

[39] F. E. Close, C. E. Thomas, O. Lakhina, and E. S. Swanson, Phys. Lett. B **647**, 159 (2007); X.-H. Zhong and Q. Zhao, Phys. Rev. D **81**, 014031 (2010); arXiv:0911.1856; D.-M. Li, P.-F. Ji, and B. Ma, Eur. Phys. J. C **71**, 1582 (2011).

[40] T. Feldmann, P. Kroll, and B. Stech, Phys. Lett. B **449**, 339 (1999).

[41] S. Esen *et al.* (Belle Collaboration), Phys. Rev. Lett. **105**, 201802 (2010).

[42] A. J. Lenz, Phys. Rev. D **84**, 031501 (2011).